Process Modeling in the Pharmaceutical Industry using the Discrete Element Method

WILLIAM R. KETTERHAGEN, MARY T. AM ENDE, BRUNO C. HANCOCK

Pharmaceutical Research and Development, Pfizer Inc., Groton, Connecticut 06340

Received 26 February 2008; revised 7 May 2008; accepted 7 May 2008

Published online 18 June 2008 in Wiley InterScience (www.interscience.wiley.com). DOI 10.1002/jps.21466

ABSTRACT: The discrete element method (DEM) is widely used to model a range of processes across many industries. This paper reviews current DEM models for several common pharmaceutical processes including material transport and storage, blending, granulation, milling, compression, and film coating. The studies described in this review yielded interesting results that provided insight into the effects of various material properties and operating conditions on pharmaceutical processes. Additionally, some basic elements common to most DEM models are overviewed. A discussion of some common model extensions such as nonspherical particle shapes, noncontact forces, and interstitial fluids is also presented. While these more complex systems have been the focus of many recent studies, considerable work must still be completed to gain a better understanding of how they can affect the processing behavior of bulk solids. © 2008 Wiley-Liss, Inc. and the American Pharmacists Association J Pharm Sci 98:442–470, 2009

Keywords: pharmaceutical engineering; powder technology; discrete element method; dynamic simulation; molecular dynamics; blending; granulation; milling; tableting; coating

INTRODUCTION

Processes involving particulate matter are prevalent throughout the pharmaceutical industry. In many cases, however, there are opportunities to improve the fundamental understanding of these processes to directly benefit equipment design, process efficiency, and scale-up. The use of various process modeling tools is becoming increasingly common and is playing a critical role in efforts to gain insight into these processes. Several computational process modeling tools are used in the pharmaceutical industry and have been reviewed recently.[1,2] These models include computational fluid dynamics (CFD), the finite element method (FEM), and the discrete element method (DEM).

Computational fluid dynamics is an Eulerian method that treats the material as a continuum and numerically solves mass, momentum, and energy balances. This approach can be extremely accurate for systems consisting of fluids, and can be extended to systems consisting of dilute solids in either of two general ways. In the Eulerian–Eulerian approach, the solids are assumed to be a second continuous phase for which the aforementioned balance equations are also solved. In the Eulerian–Lagrangian approach, the solids are modeled discretely using DEM, and these results are coupled with the CFD fluid model. For systems

Correspondence to: William R. Ketterhagen (Telephone: 860-686-2868; Fax: 860-686-7521;
E-mail: william.ketterhagen@pfizer.com)

Journal of Pharmaceutical Sciences, Vol. 98, 442–470 (2009)

of dense solids however, the material is usually assumed to be elastic or elasto-plastic, and other modeling approaches, such as FEM, are then required.

In contrast to CFD and FEM models, the discrete element method is a Lagrangian model and, as such, tracks the positions, velocities, and accelerations of each particle individually. This approach, reviewed by several authors,[3,4] is advantageous due to the high level of detail in the output describing the dynamic behavior of the particles. The particle positions and velocities can be used to calculate many particle-scale quantities of interest such as local concentrations and particle phase stresses, as well as examine particle-level phenomena such as segregation or agglomeration. While this approach does demand significant computational power, with the steadily increasing speed of computer hardware, the size of systems that can be modeled with DEM is continually increasing. Some recent DEM models simulate systems on the order of a couple hundred thousand particles.

The DEM approach is particularly beneficially since predictions can readily be made from simulation data that would be difficult, and possibly expensive, to obtain experimentally. Another strong point of DEM modeling is the ease at which parametric studies can be executed to study the effects of particle properties, process conditions, or equipment design. Further, since it is a discrete approach, particles can have a distribution of properties. Thus, the particles with in the system can have a distribution of sizes, for instance, or can even have varying material properties to model a mixture of various components. These details can generally not be addressed in continuum approaches.

This paper seeks to review the current status of DEM modeling of pharmaceutical processes. To this end, some of the fundamental aspects of DEM models are first reviewed, including the hard- and soft-particle approaches. Next, some common extensions of basic DEM models, such as the incorporation of cohesive forces, nonspherical particle shapes, and interstitial fluid effects are highlighted. This is followed by a review of recent DEM modeling work that focuses on some common pharmaceutical processes.

The Discrete Element Method (DEM)

There are four main classes of discrete element models, each with their own relative advantages and state of development. These consist of cellular automata, Monte Carlo methods, hard-particle methods, and soft-particle methods. Cellular automata are simple, deterministic models that have been used to study flow in silos,[5] down inclined chutes,[6] and in rotating drums.[7] They have also shed light on phenomena such as segregation via percolation[8] and vibration,[9] as well as the effects of nonspherical particles.[10] In this approach, particles are constrained to a lattice, and their movement is governed by simple rules established through experimental observation. While these models are extremely fast, they generally only provide qualitative predictions.

The Monte Carlo method is another approach that has been applied to model granular materials. This approach calculates the probability of a random arrangement of particles based on the energy associated with that arrangement. Like the cellular automata, Monte Carlo simulations are rather simple to implement and fairly computationally efficient. Monte Carlo techniques have been used to study several aspects of granular behavior, including vibration-induced segregation,[11,12] the effect on nonspherical particle shapes on hopper flow,[13] and the distribution of coating in film coaters.[14,15] However, the hard- and soft-particle approaches, as discussed in the next sections, are much more commonly used. These approaches are generally more flexible and typically permit a direct relation between material properties and model parameters, thereby increasing the likelihood of obtaining results that are in quantitative agreement with experiments.

Hard-Particle Approach

The hard-particle approach[16–20] assumes that particles are rigid so that collisions are instantaneous and binary. As a result, hard-particle models are generally best suited for dilute, collisional flows where these assumptions are good approximations. Hard-particle models often are embedded in event-driven collision detection schemes that increment the simulation time from one collision to the next. Consequently, hard-particle, event-driven simulations can be computationally efficient when the time between particle collisions is large.

A hybrid, hard-particle-with-overlap model has also been developed by Hopkins.[21] This hybrid model uses the hard-particle collision model described above, but integrates the particle equations of motion between collisions at a specified time

step. Thus, this is referred to as a time-driven approach. This time-driven approach can be computationally more efficient than the event-driven approach for systems containing many particles.

Soft-Particle Approach

In dense systems, the particle contacts are multiple and enduring. Therefore, the hard-particle interaction is not appropriate and the soft-particle model must be used. The soft-particle approach, originally developed by Cundall and Strack,[22] is not limited by the instantaneous contact time assumption of the hard-particle model and can therefore be used to investigate long-lasting and multiple particle contacts. This model allows for particle deformation which is modeled as an overlap of the particles. To prevent excessive errors from being introduced, the mean overlap value must be maintained to levels on the order of 0.1–1.0% of the particle size.[23] This is typically accomplished through appropriate selection of the spring stiffness. Using stiffness values that are too small will result in large overlap values, and will potentially lead to the introduction of significant error through inaccurate determination of contact forces and thus post-contact quantities such as accelerations and velocities.[24] The soft-particle model relies on a force–displacement (and/or force–displacement rate) relation to determine the interaction forces for each particle–particle and particle–wall contact. This approach proceeds via small time steps and is thus referred to as being time-driven. Accurate integration of the resulting particle equations of motion dictates a small simulation time step and, hence, long computation times. Soft-particle methods are generally utilized for dense, enduring-contact flows, such as those occurring in a hopper, blender, or pan coater.

The DEM soft-particle algorithm is relatively straightforward and is shown in a flowchart in Figure 1. At the onset of a simulation, the particle properties such as particle size distribution (PSD), density, mass, and moment of inertia are all defined. If process equipment is to be modeled, the geometry and dimensions are also defined. The particles are then inserted into the computational domain by defining a position and velocity for each, often by placing the particles on a lattice or by using a random number generator. The simulation then proceeds to a contact detection stage where all particle–particle and particle–wall contacts are identified. For each contact, the soft-particle deformation, which is modeled as an overlap, is calculated. Using the overlap values, force–displacement relations are used to calculate the forces acting on each particle. The total forces and moments acting on each particle are then summed and Newton's second law is used to calculate the translational and rotational accelerations. The time step is incremented and accelerations are integrated over time to determine updated particle velocities and positions. After measurement of any quantities of interest, such as velocity profiles, solid phase stresses, or local concentrations, the simulation repeats the contact detection for the updated particle positions and the loop is repeated.

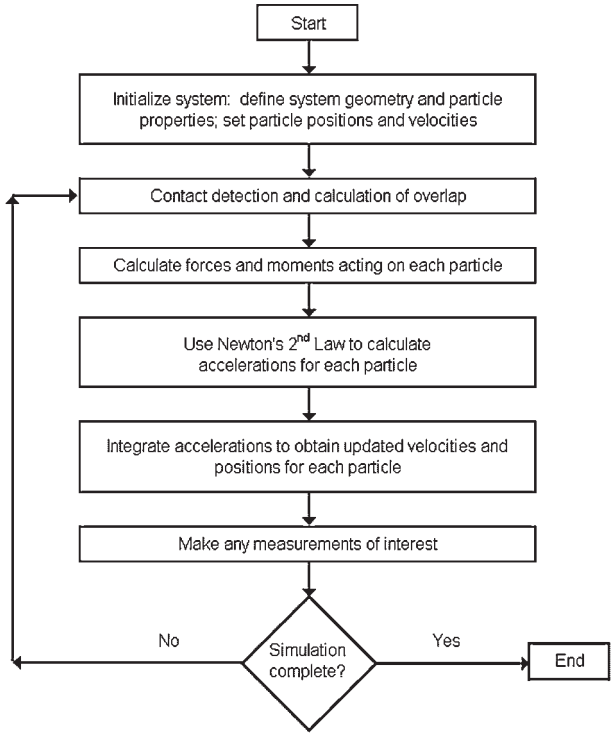

Figure 1. A flowchart of a general soft-particle DEM algorithm.

Contact models. At the heart of a DEM simulation is a particle interaction model. This particle interaction model is used to calculate the forces acting in either particle–particle or particle–wall contacts. Each of these two contact types can be resolved using the same contact model, and the material properties (e.g. coefficient of restitution, friction coefficient, *etc*.) for each contact type can differ so that dissimilar materials can be modeled. These forces are used to calculate accelerations,

which are then integrated in time for updated particle velocities and positions. The modeled forces in a soft-particle system are typically subdivided into normal and tangential components. A number of different normal force–displacement models have been proposed and these have been reviewed by several authors.[3,25–27]

One of the simplest and most commonly used normal force model is the linear spring and dashpot (LSD) model.[22,23,28–33] Here, the repulsive portion of the contact is modeled with a linear spring and the dissipative portion of the contact is modeled in parallel with a viscous dashpot. Together, these elements represent the normal portion of a contact fairly well. This commonly used model is advantageous in that the coefficient of restitution, contact time, and maximum overlap can be analytically determined. However, the resulting coefficient of restitution is not dependent on the impact velocity.

Others have modified the repulsive portion of the LSD model with a nonlinear spring following the Hertz theory of elastic contacts.[34,35] This Hertzian model is usually coupled with a dashpot to provide dissipation.[36–38] However, using this model yields a coefficient of restitution that increases with impact velocity, which is contrary to experimental data.[39] Thus, later work by Kuwabara and Kono[40] and Brilliantov et al.[41] assumed the material to be viscoelastic instead of elastic. With this modified dissipation term, the coefficient of restitution decreases with increasing impact velocity, in accordance with experimental results.[40] However, this Hertzian implementation has no intrinsic time scale for non-zero damping coefficients.[25,26] Therefore, the simulation time step must be selected by using an estimate of the maximum expected impact velocity.

Another approach was proposed by Walton and Braun[42] who assumed that materials plastically deform during contact. They developed a partially-latching, hysteretic spring model shown schematically in Figure 2 that uses one linear spring to model the repulsive force during loading, and another, stiffer linear spring to model the force during the unloading portion of the contact. This model has been used by many researchers[24,43–45] due to several advantages. First, no viscous damping coefficient is required. This is beneficial as the damping coefficients can be difficult to relate to particle properties. Second, either a constant or impact velocity dependent coefficient of restitution can be specified.

A number of tangential force–displacement models of varying complexity have also been proposed and reviewed by several authors.[3,25,26] One of the simplest models was first introduced by Cundall and Strack[22] and subsequently used by several others.[46–48] Here, the tangential force is modeled with a linear spring where the associated displacement is integrated from the relative velocity at the contact point. This tangential force determined by the spring is limited by the Coulomb criterion, which specifies that the maximum frictional force is proportional to the normal force, where the coefficient of friction is the proportionality constant. This tangential force model is an attractive choice because it is relatively

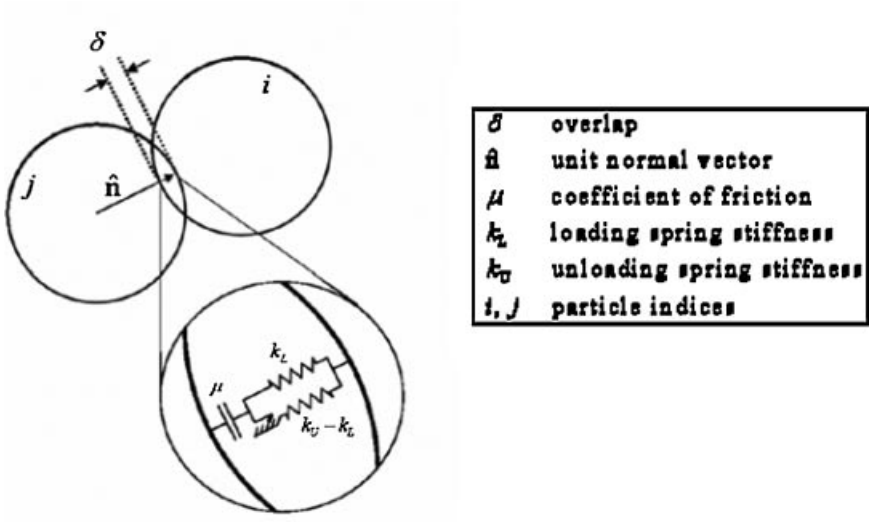

Figure 2. A schematic of the Walton and Braun[42] hysteretic spring model.

easy to implement and reproduces experimental observations fairly well.[25] It does however require a tangential displacement value to be stored in memory for each contact.

Other tangential force models have been based on the detailed analysis of frictional, elastic spheres by Mindlin and Deresiewicz[49] which specifies that the tangential force is dependent on the loading and unloading history of the contact. The full model considers eleven different loading/unloading possibilities, but generally, only two are considered in DEM implementations. The implementation of this model is significantly more complex than the Cundall and Strack model discussed previously, but compares only slightly better with experimental results, as reported by Schäfer et al.[25] Despite the additional complexity of this tangential model, it has been used frequently by several authors.[42–45,50]

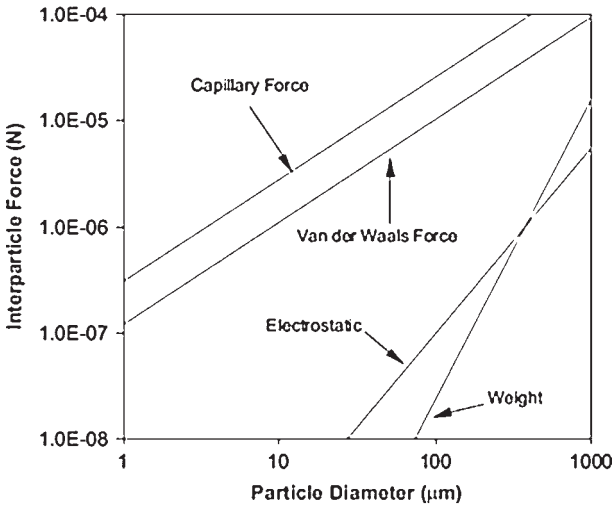

Figure 3. A comparison of the magnitude of interparticle forces for varying particle diameters. This figure is reprinted from Zhu et al.[4] with permission from Elsevier.

Model Extension

Historically, discrete element models have considered only cohesionless particles of circular (in 2D) or spherical (in 3D) shape, while neglecting the effects of interstitial fluids. These simplifications have been made primarily due to the complexities of contact detection and the extensive computational power required to model more complex systems. However, as the speed of computers has increased, the scope of systems than can be modeled in a reasonable amount of time has similarly increased. Today, it is not uncommon for researchers to use DEM to model systems with secondary forces such as cohesion, nonspherical particle shapes, or interstitial fluid effects. Each of these extensions will be discussed in the following paragraphs.

Noncontact Forces

Noncontact forces due to capillary cohesion, electrostatics, or van der Waals interactions may significantly affect the behavior of bulk solids, especially for systems with small particle sizes or where moisture is present. Figure 3 shows the magnitudes of these forces and how they become quite significant relative to particle weight as the particle diameter decreases. The importance of these forces has been reviewed by Seville et al.[51] and the application of such forces in DEM models has been reviewed by Zhu et al.[4] Cohesive forces strongly affect the flowability of powders[52] and can lead to ratholing and arching during hopper discharge, blockage of pneumatic conveying lines, as well as agglomeration and caking of powders.[53] Additionally, cohesive forces can significantly affect fluidization processes by causing agglomeration and subsequent defluidization.[54] While cohesive forces are significant in most powders, many DEM models have not included cohesive forces.[55] Thus, further study of cohesive systems is clearly needed to gain a better understanding about these effects.

Some of the simplest methods to model cohesion use a proportionality constant to predict the attractive force between particles. These methods predict the cohesive force by a spring constant,[56,57] a constant proportional to particle weight,[58–60] a square-well potential,[53,61–63] or by assuming the cohesive force is proportional to contact area.[64] Each approach is relatively simple to implement, but uses constants that may not be directly related to experimentally measurable values.

A more rigorous treatment models cohesion with pendular liquid bridges. The capillary force of a liquid bridge is specified by the Young–Laplace equation; however, this equation generally cannot be solved analytically. Thus, Fisher[65] and, more recently Lian et al.,[66] assumed a torodial liquid bridge shape, which allows for an estimation of the capillary force. Lian et al.[66] showed that the error associated with this torodial assumption is less than 10%. While the expressions based on the torodial assumption permit an estimation of the capillary force, they are not

explicit and so an iterative scheme must be used. This approach has been used in several DEM models to study the fundamental behaviors of cohesive materials in shear flow,[52] during packing,[67] and while forming repose angles,[55] as well as in more complex systems such as a vibrated bed,[68] rotary drum,[69] and high-shear granulator.[70] Mikami et al.[54] developed regression expressions that provided an explicit calculation of the force as a function of the separation distance, and therefore provided a more amenable method for incorporating cohesive forces into DEM models. These expressions were later extended to the polydisperse case.[71] Due to the ease of implementation, these regression equations have been used to incorporate cohesive forces in studies of uniaxial compression,[71] shear flow,[72] fluidization,[54,73] and hopper discharge.[74]

Other attractive forces such as van der Waals forces and surface adhesion have also been incorporated in to DEM models. van der Waals attractive forces have been added to study packing and rearrangement of fine particles[75] as well as fluidization.[76–78] Thornton and Yin developed a theory for contacts in the presence of adhesion,[79] and later applied this model in the study of agglomerate fracture.[80] A few researchers have recently applied discrete element models to colloidal systems as well. For these systems, a DLVO potential, based on the theory of Derjaguin, Landau, Verwey, and Overbeek[81,82] is often employed. This DLVO potential is based on the cumulative effects of electrostatic repulsion and van der Waals attractive forces. Additionally, an attractive force, based on the theory of Johnson–Kendall–Roberts (JKR),[83] is also included in some models for colloidal systems.[84–86]

Particle Shape

Many studies of granular materials using DEM have modeled particles with spheres in 3D or disks (circular shapes) in 2D. The use of these simple shapes allows for straightforward contact detection and contact resolution. However, these sphere/disk systems are often too idealized to accurately model some phenomena exhibited by real granular materials. For instance, it has been shown that spherical particles have a smaller angle of repose[87,88] and a reduced strength[89,90] as compared to nonspherical particles. The underlying cause is that the rotation of spheres is only resisted by frictional contacts with neighboring particles whereas for nonspherical particles, rotation tends to be inhibited by mechanical interlocking.[91–93]

Several different methods have been used in an attempt to reduce the rotational freedom of spheres/disks within DEM models. Ting and Corkum[94] artificially increased the particle moment of inertia thereby reducing particle rotation. Others have damped[95] or completely fixed[96–98] particle rotation. Another approach incorporates a rolling resistance.[38,99–101] This approach shows promise however, it also introduces additional parameters to the model via rolling resistance coefficients.

Due to the aforementioned differences between experimental particles and DEM models of spheres, a common extension of the basic, noncohesive, sphere-based DEM models is to incorporate nonspherical particle shapes. For systems of spheres/disks, contact detection and contact resolution are relatively straightforward. However, for nonspherical particles, these calculations can become quite complex. A wide range of nonspherical particles have been implemented in DEM models, and many of these have been reviewed by Džiugys and Peters[102] and Hogue.[103]

One of the simplest approaches to model nonspherical particles is by "gluing" two or more spheres or disks together in either a rigid or flexible manner. This clustering approach has been commonly used in 2D with disks[87,88,104,105] and in 3D with spheres.[50,106–113] This approach retains the relative simplicity of contact detection and contact calculation associated with spheres or disks. Additionally, arbitrary or nonsymmetric particle shapes can be modeled. However, a drawback is the difficulty in modeling shapes that have sharp edges.[114,115] Also, a potential disadvantage is the roughness of the resulting particles if they consist of only a small number of spheres/disks. It has been shown that the dynamic behavior of a sphere-cluster particle may be significantly different than that of the smooth particle it is intended to represent.[116]

A similar method uses the idea of mathematical dilation[117] to create spherocylinders and spherodisks.[13,118–123] These so-called dilated shapes are created by placing a sphere with a fixed diameter at every point on some basic geometric shape. A spherocylinder is created by dilating a line segment with a sphere while a spherodisk (a 3D disk) is created by dilating a 2D disk with a sphere. Thus, each particle is modeled by an infinite collection of spheres, resulting in a smooth particle surface. However, the contact detection

for dilated shapes becomes somewhat more complicated than that for spherical particles.

Another class of shapes is those that can be mathematically defined. Most commonly, these include ellipses in 2D[89,90,102,124–127] and ellipsoids in 3D[92,128–130] as defined by

$$\left(\frac{x}{a}\right)^2+\left(\frac{y}{b}\right)^2+\left(\frac{z}{c}\right)^2-1=0 \quad (1)$$

where a, b, and c define the lengths of the three principle axes which are aligned with the local x, y, and z coordinates, respectively. Superquadrics,[131,132] the general class of shapes to which ellipses belong, have also been used in 2D[23,130,133,134] and 3D[135] to represent nonspherical particles. The shapes of several superquadrics, shown in Figure 4, are mathematically given by

$$\left|\frac{x}{a}\right|^\alpha+\left|\frac{y}{b}\right|^\alpha+\left|\frac{z}{c}\right|^\alpha-1=0 \quad (2)$$

where the exponent $\alpha>0$ characterizes the blockiness of the particle. For $\alpha=2$, the equation of an ellipsoid is recovered. For increasing values of α, the corners begin to sharpen and the particle becomes increasingly blocky. Superquadrics are advantageous since they can algebraically model a wide variety of particle shapes with various values of the exponent α and the aspect ratios as determined by a, b, and c. Additionally, the normal vector is algebraically defined. However, for these shapes, contact detection is usually prohibitively slow as the intersection of two nonlinear functions must be calculated.

Polygonal particles are another class of particle shapes popular in the field of geomechanics. Arbitrary or symmetric polygons have been modeled in 2D[48,115,134,136–140] and in 3D.[141–145] Additionally, polygons constructed of beams and triangular elements have also modeled in 2D.[114,146] Polygonal particles pose certain

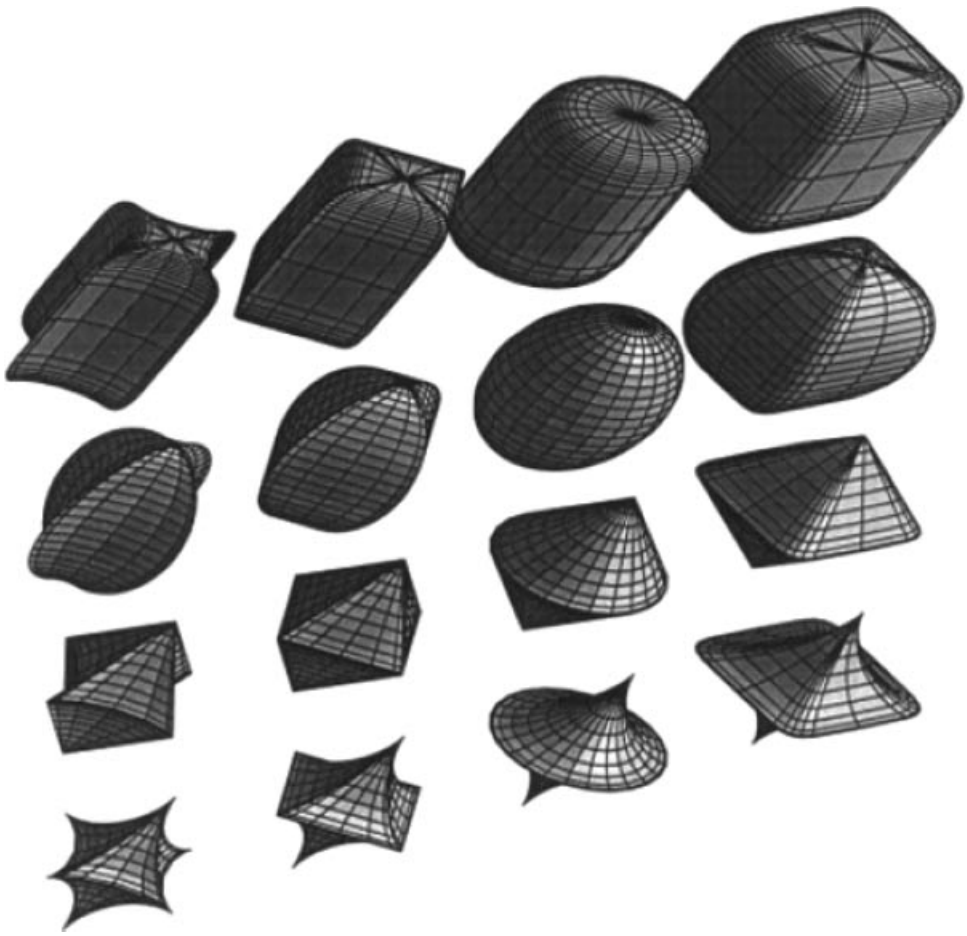

Figure 4. Images showing some possible particle shapes using 3D superquadrics. This figure reprinted from Hogue[103] with permission from Emerald Publishing Group.

difficulties surrounding contact resolution involving corners and edges. Additionally, modeling round or smooth particles with this method is inefficient due to the large number of facets involved.

Potapov and Campbell[147] developed another shape representation for 2D systems. They connected four circular arcs in a continuous manner to create an oval shape. This representation allows for nonround particles to be modeled with only a small increase in the computational effort. Additionally, this approach of connected arcs can be extended to model any other 2D polygon (e.g. triangle, square, pentagon, *etc*.). A drawback of this method is that there is no simple implementation of this general scheme in 3D. One exception is the case of ovals, which have been extended to 3D ovoids[148–150] by rotating the oval around an axis of symmetry.

Another approach is the discrete function representation for 2D shapes, as defined by Williams and O'Connor.[137] This method discretizes the surface of an arbitrarily shaped particle based on a single parameter resulting in a list of vertices that can easily be searched for contacts. One example is given by Hogue and Newland[151] who discretized particles via a polar representation. Here, the surface of a given particle is specified by a polar angle and radius for several vertices on the surface. This approach was also used by Wu and Cocks in die filling investigations.[140,152] An extension to 3D has also been proposed[103] where two parameters are used to discretize the particle surface. This discrete representation approach can represent a wide variety of arbitrary shapes that can be either convex or concave, smooth or angular, and elongated or compact.

A final particle shape worth mentioning is that of a round, bi-convex tablet.[116,153] This shape is defined mathematically by the intersection of one small sphere that defines the tablet band and two larger spheres that define each of the convex caps. This shape is advantageous in that it precisely models the shape of interest, and it does so in a computationally efficient manner.

While each of these nonspherical shape representations has its relative merits, it is important to consider the increase in computational time associated with each method. Some authors have reported the relative differences in run time for various shape representations[116,147] and several observed computational times are summarized in Table 1. While these results are not comprehensive, they show that sphere clusters, continuously joined arcs, and bi-convex tablet shapes all require only modest additional computational effort beyond that of spherical particles. In contrast, the computational cost for polygons and superquadrics may be on the order of two to ten times that for a system of spheres. The computational times presented in Table 1 are stated relative to the case of disks/spheres in an effort to eliminate any differences between number of particles, the length of time simulated, and the computational

Table 1. Computational Times for Various Particle Shape Representations as a Multiple of the Time Required for Disk-Shaped or Spherical Particles

Dimensionality	Shape	Increase in Computational Time Over that for Disks	References
2D	Quasi-triangle	1.7	147
2D	Quasi-square	1.8	147
2D	Superquadric	3	134
2D	Square	3.9	147
2D	Superquadric	12	147

Dimensionality	Shape	Increase in Computational Time Over that for Spheres	References
3D	10 sphere cluster	1.1	116
3D	26 sphere cluster	1.2	116
3D	Biconvex tablet	1.5	116
3D	Ovoid	2	149
3D	Superquadric	~2–3	33
3D	66 sphere cluster	2.2	116
3D	178 sphere cluster	6.3	116

resources utilized. However, differences in the contact algorithm, the degree of optimization, or other factors may still result in widely varying computational times (e.g., the differences for 2D superquadrics).[134,147]

Fluid Effects

The effects of interstitial fluids are neglected in many DEM models. For many systems, such as those with relatively large particles, typically greater than 500 μm, this assumption is usually satisfactory.[154] However, for systems with fine particles, it may be critical to include interstitial fluid effects to obtain accurate model predictions. Additionally, for processes such as fluid bed drying and pneumatic transport, the fluid phase must be modeled.

The inclusion of such effects is currently an emerging area of study where an Eulerian CFD model is coupled with a Lagrangian DEM model. Thus, the fluid phase is treated as a continuum, while the particulates are modeled as discrete elements. Typically, these studies are carried out with a CFD model coupled with a DEM model using either the hard-[155] or soft-particle[156] approach. Further details of these coupled models are described in several excellent reviews.[4,157]

Several pharmaceutical processes have been studied using these coupled models. For example, air effects have been included in the study of fluidized beds,[155,156,158–162] spouted beds,[163,164] and the effects of cohesion therein.[54,58,165] The presence of air has also been shown to affect the die filling process.[140,166] Finally, the incorporation of air effects is required in pneumatic conveying models.[167–169]

Validation of DEM Models

The verification and validation of computational models are of utmost importance. The term verification is used to describe the process of ensuring that the numerical solutions are in fact an accurate solution to the model. Thus, this issue addresses the computational implementation of the mathematical equations. The term validation describes the process by which the accuracy of a model's predictions are compared with experimental data. This area has been widely discussed in the CFD literature via, for example, textbooks,[170] policy statements,[171,172] and review articles.[173] However, the verification and validation of DEM models does not appear to be as rigorous and the procedures certainly are not as well defined. This is attributable primarily to the difficulty in obtaining experimental data with which to compare. The extent and methods of verification and validation used by researchers vary widely, and often these are not fully described in the literature. A notable exception is the work of Asmar et al.[56] that outlined several fundamental, two-body contacts to verify their DEM model. It was also suggested that these results be used as a benchmark for verification by other researchers.

Discussions of validation studies have appeared considerably more frequently in the literature than those regarding verification. Most validation studies for DEM models have been qualitative and rely on visualization of experimental flows on the surface or at a transparent wall. For example, experimental observations have been used to qualitatively validate flow in a rotating cylinder,[174–176] fluidized bed as shown in Figure 5,[162] tumbling mill,[177] vibrated bed,[178] and during heap formation.[179] However, the opacity of bulk solids limits the applicability of these visualization techniques to quasi-2D systems (e.g. a thin slice of a cylindrical rotating drum). Thus, validation studies of 3D systems that rely on visualization of the material on a free surface or at a transparent wall in order to assess particle phenomena, such as the flow pattern, occurring within the interior may be tenuous.

One approach to validation for 3D systems relies on making measurements of macroscopic quantities. For example, the measurement of hopper discharge rates[180,181] can be compared to the well established Beverloo correlation.[182] Figure 6 shows one such comparison with excellent agreement between the DEM and Beverloo predictions. This hopper discharge rate is an example of a simple benchmark test for model validation. Researchers have also measured other macroscopic quantities for validation including the extent of segregation of bidisperse material during hopper discharge[183] and the power draw in a tumbling mill.[177]

Tomographic techniques have also been developed towards validation of 3D granular systems. These techniques are nonintrusive and are not hindered by the opacity of solids. Therefore, they are ideal methods to probe the internal microstructure and particle velocities within 3D systems. Nuclear magnetic resonance (NMR)[184] has been used for validation of a long rotating cylinder.[109,185] Also, the blend uniformity in a

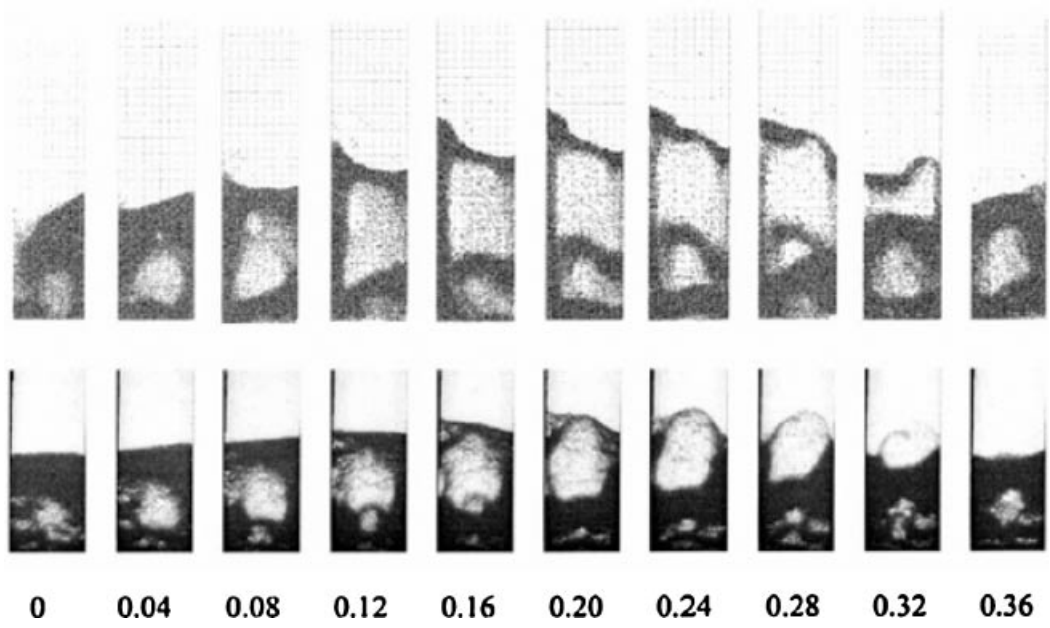

Figure 5. Comparison of fluidized bed simulations (upper) and experiments (lower) at the given times in seconds. This figure is reprinted from van Wachem et al.[162] with permission from Elsevier.

hopper has been quantified using gamma-ray tomography[186] and the packing of particulates has been examined using X-ray microtomography.[187,188] The positron emission particle tracking (PEPT) technique[189] has also been used to probe various equipment including high-shear mixers,[190,191] a V-blender,[192] a ploughshare mixer,[193] and fluidized beds.[194,195] This method tracks a single radioactively labeled particle for times on the order of several minutes to an hour to compile the internal flow velocities, which can then be compared with DEM predictions.

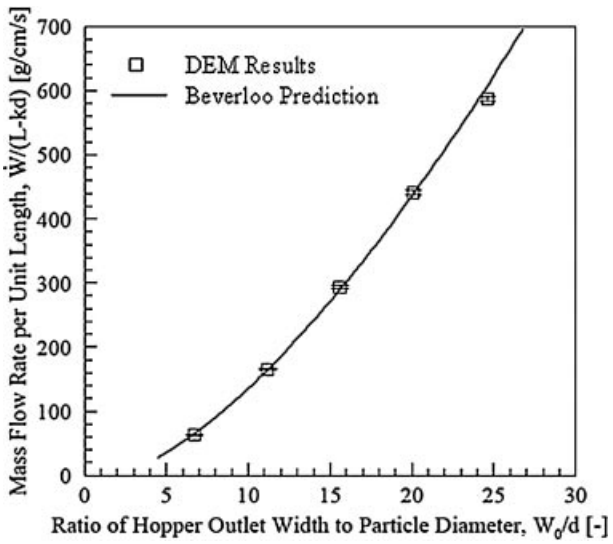

Figure 6. DEM predictions of the mass discharge rate per unit length of a monodisperse material in a flat-bottomed, wedge-shaped hopper as a function of the ratio of outlet width to particle size W_0/d.[181] The line indicates the discharge rate as predicted by the Beverloo correlation[182] modified for wedge-shaped hoppers.[298]

Limitations of DEM Models

The discrete element method is an emerging area of computational modeling. The primary limitation of the technique is its inherent computational intensity. Since the DEM approach tracks each individual particle, any increase in the number of modeled particles, N, increases the computational time, which typically scales as $N\,\mathrm{Log}(N)$. This effectively limits the number of particles that can be modeled. The number of particles in a system of volume V and relative density ϕ is given by

$$N = \frac{6V\phi}{\pi d^3} \sim \frac{V}{d^3} \tag{3}$$

where d is the particle diameter. Thus, as the volume of a system increases or the particle diameter decreases, the number of particles increases significantly. This is illustrated in

Table 2. The Approximate Number of Particles in a 1 L Volume for the Given Particle Diameter and Assuming a Relative Density of 0.625

d (μm)	N
10	10^{12}
20	10^{11}
50	10^{10}
100	10^{9}
200	10^{8}
500	10^{7}
1000	10^{6}
2000	10^{5}
5000	10^{4}

The dark shading indicates system sizes that are typically inaccessible with current DEM models and computational power. The unshaded areas are accessible, and the light shading indicates an intermediate regime.

Table 2 where the approximate number of particles in a 1 L volume is tabulated for the given particle diameter assuming a relative density of 0.625. Typical DEM models at present are capable of modeling on the order of 10^5 particles. Thus, to model a 1 L system on a one-to-one basis, the particle diameter could be no smaller than approximately 1–2 mm.

While the above example demonstrates that only select systems with a small number of particles can be modeled on a one-to-one basis, there is utility in modeling larger systems. For these systems with large numbers of particle required, DEM approaches can still be quite useful in elucidating qualitative trends and learning more about particulate behavior and how it is affected by certain particle properties, process parameters, and equipment design.

For those systems involving a large number of particles, several different approaches have been taken to ease the required computational effort. One frequent approach takes advantage of symmetry within a system of interest thereby allowing for the use of periodic boundary conditions.[24,70,101,196] The use of such boundaries reduces the size of the computational domain and thus, the number of modeled particles, without affecting the measured results. A second approach artificially increases the size of the modeled particles. For example, 10 μm particles could be approximated with 10 mm particles in a DEM model which would reduce the total number of particles within the system for a given solids volume. However, caution must be exercised using this approach as particle-level phenomena may differ between the two scales. Further, as in the example cited above, effects such as cohesion are usually quite significant for 10 μm particles but typically insignificant for 10 mm particles. Finally, a third approach partitions the computational domain into smaller regions, but still models the flow in each region. The flow in each region can then be modeled with DEM sequentially on a single computer[197] or distributed to several computers (i.e. parallelized).[23] In contrast, others have only used DEM to model certain regions of interest and have used other approaches such as FEM[198] or stochastic methods[199] to model the flow in the bulk of the domain.

In addition to the significant effect that the number of particles has on the computational time, certain complexities added to the model can also increase the computational time considerably. Such complexities include nonspherical particle shapes, as discussed earlier and summarized in Table 1. Additionally, the inclusion of secondary forces, such as cohesion, or the coupling of the DEM model with CFD to capture interstitial fluid effects will also necessitate a longer computational time.

There are also some other technical concerns regarding DEM models. One common concern is the difficulty associated with sufficiently validating the models. An advantage of DEM is that it can probe complex systems where experimental measurements are difficult or expensive to obtain. This becomes a detriment when it comes to validating the model experimentally, as the necessary measurements may not be available. However, as discussed in the preceding section, researchers are continually devising new techniques and using new experimental tools to obtain measurements for validation. Another common concern is the use of spherical shapes to represent nonspherical granular materials. While this is a typical assumption used to reduce the computational time requirements for a given simulation, results from experiments and DEM simulations have shown that nonspherical particles can significantly affect particulate flow behavior. This is also an ongoing area of research with a focus on developing fast contact detection algorithms for nonspherical particle shapes.

APPLICATION TO PHARMACEUTICAL PROCESSES

A wide variety of particle handling and processing equipment is typically used in the pharmaceutical

industry. The discrete element method has been used with good success to model many of these processes resulting in a better understanding of these systems. In the following sections, highlights of that body of work are presented in the areas of transport and storage, blending, granulation, milling, compression, and film coating.

Transport and Storage

The transport and storage of bulk solids has been comprehensively studied using DEM. Much of the research has focused on relatively simple geometries to permit examination of the underlying granular physics. For instance, numerous studies have examined the solid phase stresses in simple shear flow with periodic boundaries.[24,32,42] Additionally, others have studied the stresses and solids fractions within flows down an incline,[38,50,200] and during the formation of a heap.[48,201,202] In addition to these relatively simple geometries, more complex systems such as hoppers, pneumatic conveying lines, and screw conveyors have also been studied using DEM.

The flow from a hopper is frequently studied due to the prevalence of hoppers in all solids handling industries. Bulk quantities such as the mass discharge rate[47,203–206] are often measured and compare well with empirical correlations such as that proposed by Beverloo.[182] Cleary and Sawley extended this work to show how nonspherical particles affect the hopper flow rate.[23] Other work, shown in Figure 7, reported how bidisperse materials segregate during discharge due to differences in particle size.[101,183] Due to the discrete nature of DEM models, the positions and velocities of each particle are known at every time step. This information has been used to examine features within the granular bed that may be difficult to obtain experimentally. For example, the granular microstructure[186,206] and the internal stresses and/or flow fields[31,46,207–209] have been obtained for various hopper flow systems. Finally, other work has examined unusual hopper geometries,[44] the stresses acting on the hopper walls,[47,203,204,208] and the effects of hopper vibration,[210,211] flow promoting inserts,[197] and interstitial air on hopper discharge.[154]

Discrete element models have also been coupled with computational fluid dynamics (CFD) to study the effects of interstitial fluids. One system for which these coupled models are often applied is pneumatic conveying. In some of the earliest work, Tsuji et al.[167] developed a model for the pneumatic transport of cohesionless material in a horizontal pipe. Later, other work included extensions for heat transfer,[212] attrition,[213] and electrostatics.[214,215] Other researchers have studied the saltation of solids that occurs in low-velocity flows when the particles fall out of suspension,[216] and developed phase diagrams to describe the various flow regimes observed in vertical and horizontal pipes.[168] Further work has examined flow regimes in inclined pipes, and found good agreement with results from an experimental system.[169]

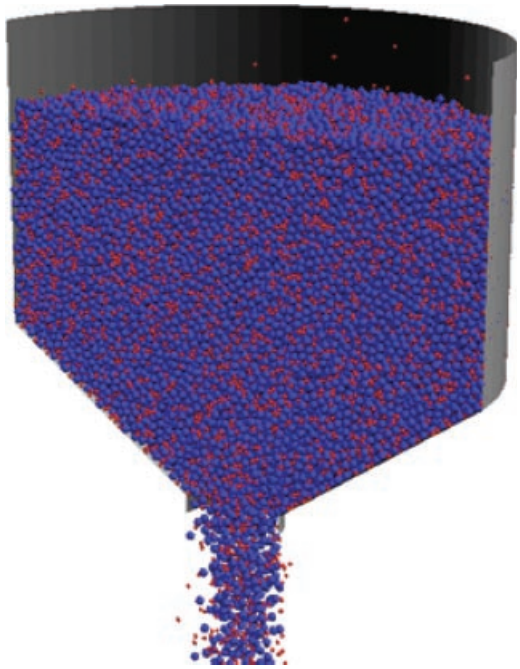

Figure 7. Snapshot of a hopper discharge simulation examining the extent of segregation of bidisperse material during discharge.[183]

Another solids transport system modeled via DEM is the screw conveyor. Such models have studied the conveyance of spherical[33,217] and nonspherical particles.[135] Results have shown good agreement with established empirical correlations for transfer velocity and power.[217] Figure 8 shows an image from a screw conveyor simulation where segregation of polydisperse material is observed to occur after only two revolutions of the screw. Other related work has examined solids feeding and conveying within a single-screw extruder[218] and mixing within a twin-screw extruder.[219]

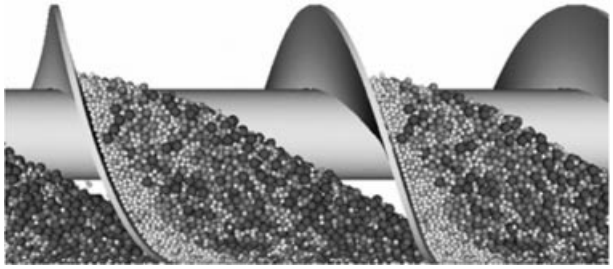

Figure 8. A snapshot from a simulation of a screw conveyor where the particles are shaded according to their diameter. Size segregation is apparent here after only two screw revolutions. This figure is reprinted from Cleary[33] with permission from Emerald Group Publishing.

Blending

Blending operations are one of the most common applications of DEM models and much of the recent work is highlighted in a review by Bertrand et al.[180] A number of different mixing systems have been modeled including V-blenders, tote blenders, and bladed mixers. However, one of the most frequently studied mixing systems is that of a rotating drum. For example, studies of rotating cylindrical drums, reviewed by McCarthy et al.,[220] typically focus on mixing and segregation in the radial[43,69,196,221–224] and axial[175,196] directions. Other studies have reported measurements of the velocity field,[109,175,224,225] angle of repose,[109] and surface shape.[226] This simple geometry produces a steady flow where the mixing rate and mechanisms can be readily studied.

The mixing in other rotating devices has also been studied. The study of twin shell or V-blenders has focused on the flow and mixing mechanisms,[45] the sensitivity to simulation parameters,[192] different fill patterns,[227] and the extent of mixing over long times.[228] The effectiveness of a V-blender has also been compared to a double cone blender.[45] Other work has focused on various tote blenders. Computational mixing results in a pyramidal tote blender have compared favorably to 1:1 scale experiments with glass beads.[229] The mixing mechanisms in a conical tote blender were examined as a function of percent loading.[230] Other work compared mixing in a conical tote blender with that in a V-blender.[227] Further, a study of baffles in a cylindrical tumbler rotating on an axis perpendicular to that of the cylinder has shown the importance of baffle design.[231]

Other studies have examined various mixing equipment with an impeller, such as the vertical axis cylindrical mixer with a rotating blade shown in Figure 9. Stewart et al.[190] simulated the mixing in such a device and compared the results with experimental measurements obtained via positron emission particle tracking. The overall flow was successfully predicted by DEM, but the model did not closely predict the velocities in all regions of the bed. Later work by the same authors examined the granular microstructure during mixing.[232] Others have determined an optimal fill level[233] and examined the effect of different impeller shapes.[191]

Terashita et al.[234] studied the particle segregation due to density differences while Zhou et al.[235] extended this work and examined segregation due to both density and size differences. Finally, a hybrid model was proposed and implemented in a horizontal convective mixer with an impeller.[199] This hybrid model employs DEM to model regions of high shear and a stochastic compartment model for the remainder of the domain.

Two other mixing devices have also been investigated with DEM. A helical ribbon blender has been analyzed,[180,236] and results show how the flow patterns and extent of mixing are affected for various rotational speeds and fill levels.[236] Further, the suitability of static mixers for bulk solids has been reviewed[237] and studied using DEM.[238] The observed flow regimes from the DEM study compared well with previous experimental results.

Granulation

The granulation process and the many approaches to modeling it have been summarized in a review by Cameron et al.[239] While a population balance models have played a key role in granulation process modeling, discrete element models have also played a small, yet significant part of this modeling effort thus far. Much of this DEM work has occurred only in the past few years.

One approach used in DEM modeling of granulation was taken by Gantt and Gatzke.[240] In this work, a high shear granulator was modeled using a DEM model that incorporated three key mechanisms of granulation: coalescence, consolidation, and breakage. The rates of each mechanism are directly simulated and incorporated to model a dynamic particle size distribution (PSD). The results from this DEM model were in good agreement with previous approaches using

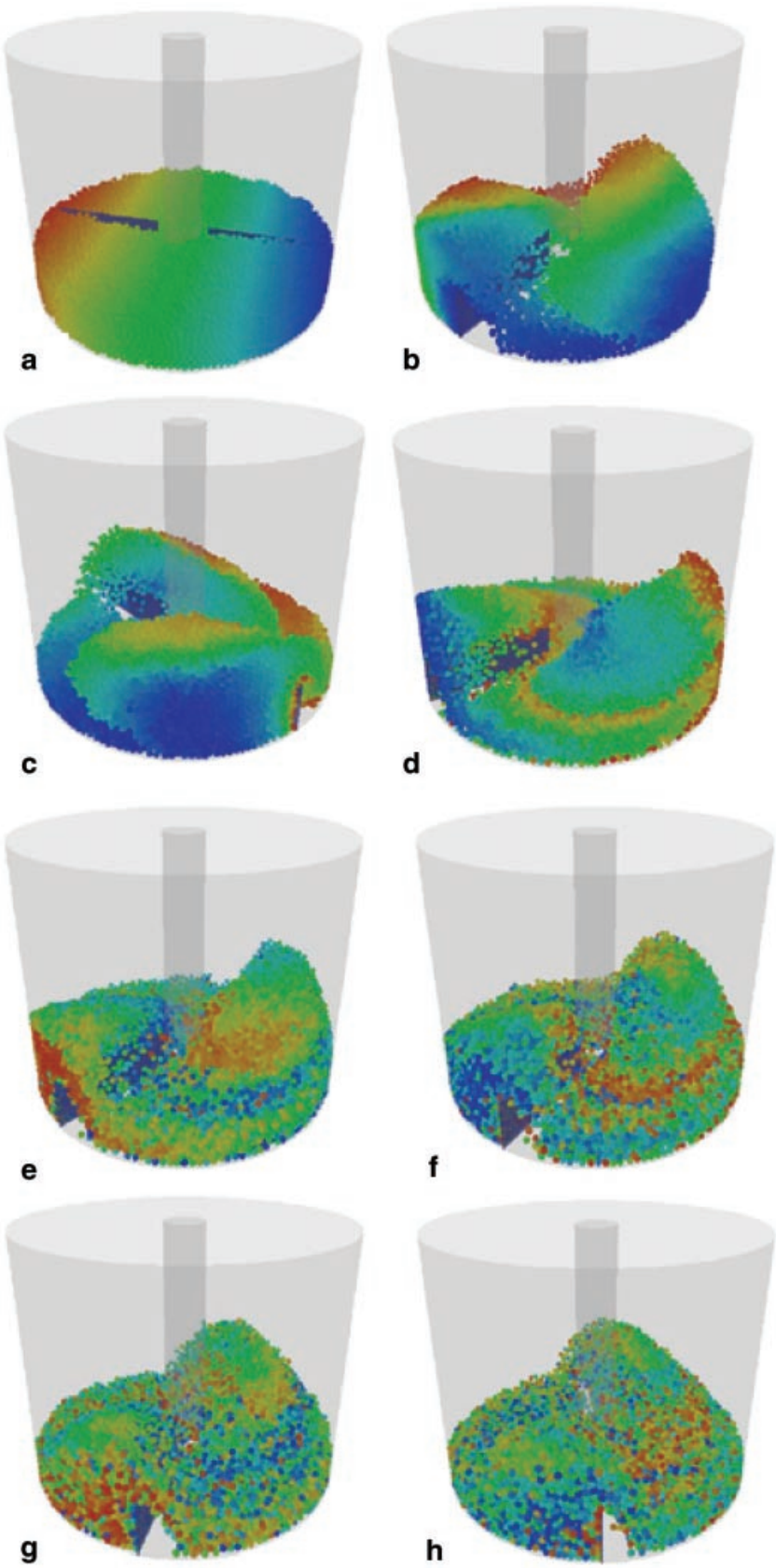

Figure 9. Images from a DEM simulation of a bladed mixer after (a) 0.1 s, (b) 0.4 s, (c) 0.7 s, (d) 1 s, (e) 2 s, (f) 3 s, (g) 4 s, and (h) 5 s. This figure is reprinted from Bertrand et al.[180] with permission from Elsevier.

population balances;[241] however, the DEM approach also has the ability to model dynamic operating conditions.

Gantt et al.[242] used another approach where a DEM model with periodic boundary conditions was used to represent flow in a high-shear granulator. The particle collision statistics compiled by the DEM simulation were used to develop a coalescence kernel. This kernel was then used with a Monte Carlo method to solve a multidimensional population balance.[243] Good agreement with experiments was observed, but could be improved with better incorporation of material properties such as wet granule yield strength, Young's modulus, and asperity size.

The agglomeration of particles is typically modeled using one of two methods. In the first method, the discrete elements always represent the primary particles.[244] Thus, the agglomerates many consist of many discrete elements. This method retains information on agglomerate porosity and morphology, and subsequent breakage is readily modeled.[245] This approach has also been used to study the impact of two agglomerates at different impact velocities and binder fluid properties.[246] In the second method, agglomerates are modeled as a single discrete element, the mass and volume of which are determined from those of the constituent primary particles.[247] This method allows for the simulation of larger systems since fewer discrete elements are required. The major disadvantage or limitation is that agglomerate breakage cannot be readily modeled using this method.

A wide variety of different granulation equipment has been modeled with the DEM approach. Talu et al.[248] modeled agglomeration and breakage in 2D shear flow of a mixture of "wet" and "dry" particles showing the effect of the amount of liquid binder, the Stokes number, and the Capillary number on the PSD. Muguruma et al.[70] modeled the centrifugal tumbling granulator shown in Figure 10 where the liquid was uniformly distributed. The resulting velocity profiles were in agreement with experimental data using glass beads of same size. Mishra et al.[249] examined the agglomeration of particulates in a rotary drum with a model that included a spray zone and also considered the drying of particles. Granulation in fluidized beds has also been modeled. Goldschmidt et al.[247] modeled granulation in a top-spray fluidized bed. In that work, both the particles and droplets were modeled using the hard-particle approach. Results showed the development of the PSD over time as a function of the fluidization velocity and the spray pattern. In a similar study, Link et al.[250] examined granulation in a spout fluidized bed.

Dry granulation techniques have also been explored by a few authors with mixed success thus far. Odagi et al.[251] modeled a roller compaction process using DEM, but the pressures in the nip region were several orders of magnitude smaller than experimental values. In contrast,

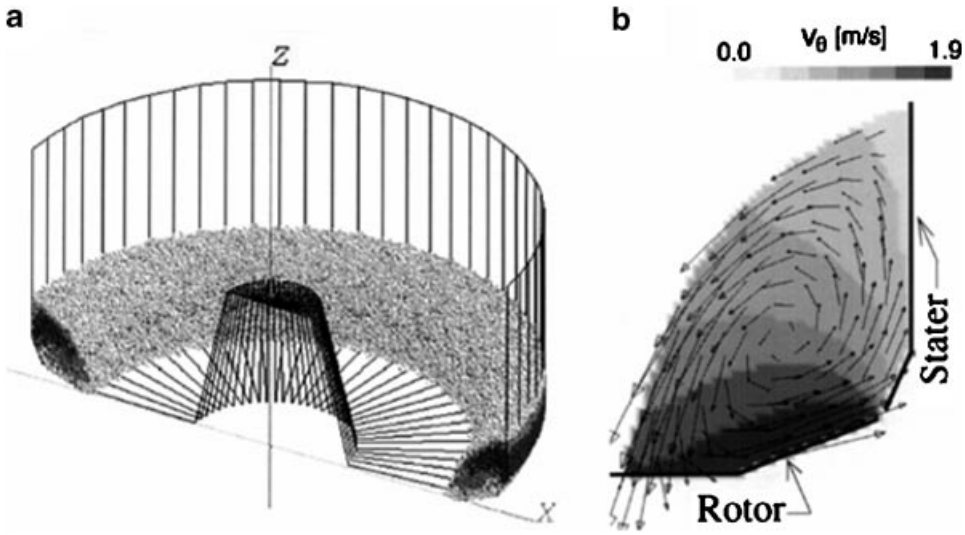

Figure 10. A DEM model of a centrifugal tumbling granulator with (a) particle positions and (b) particle velocity profiles. This figure is reprinted from Muguruma et al.[70] with permission from Elsevier.

Dec et al.[252] modeled roller compaction using the finite element method with good success. Thus, in cases where large pressures are present, such as the nip region of a roller compacter, a continuum model may be superior to DEM approaches. Additionally, Horio[253] examined dry granulation in a fluidized bed. This so-called pressure swing granulation relies on the intrinsic cohesivity of particles to form relatively weak agglomerates.

Milling

The discrete element method approach to modeling comminution devices has provided insight into particle fracture patterns and the change in PSD. This work is usually focused on one of two processes. The first is the study of particle fracture and/or attrition while the second involves the dynamics of materials within the milling device. Several researchers examining particle fracture have developed models exploring the effect of impact velocity and bond strength on fracture. The approaches taken to model breakage are varied. One approach, originally developed by Potapov and Campbell,[254] creates a nonporous, 2D agglomerate of Delaunay triangles[254–256] or arbitrary polygons via a Voroni tessellation.[255–257] Agglomerate fracture, as shown in Figure 11, occurs when the tensile strength of the glued joints is exceeded. In another approach, agglomerates are created with randomly arranged spherical particles and held together with surface adhesive forces.[80,258–261] Breakage of the agglomerate results when tensile forces between spheres exceed the surface adhesive forces. The mode by which agglomerates break is dependent on both the agglomerate strength and the impact velocity where large velocities may cause shattering, but smaller velocities may only lead to a plastic deformation of the agglomerate. A DEM and experimental study of weakly agglomerated

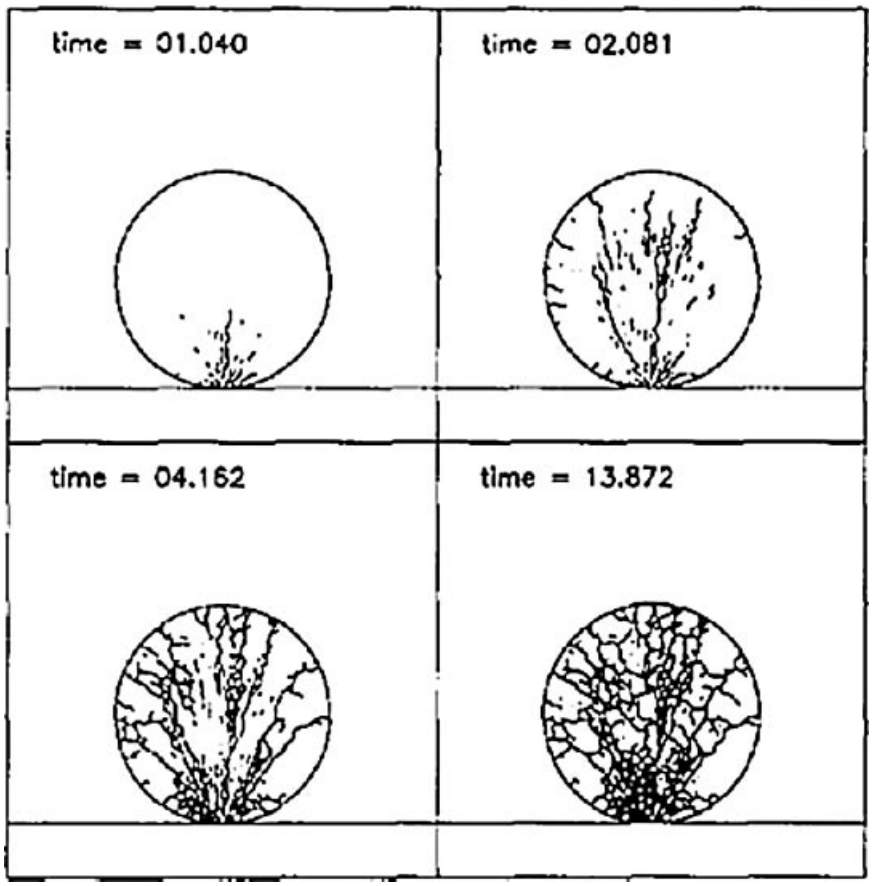

Figure 11. Images from a DEM model showing the impact and fracture of a single particle consisting of 2043 triangular elements. This figure is reprinted from Potapov and Campbell[254] with permission from Elsevier.

lactose particles has shown that they tend to deform plastically rather than fracture.[258]

A different approach estimates the particle breakage using an analytic model. For example, Neil and Bridgwater,[262] following the work of Gwyn,[263] attempted to characterize attrition with a single parameter irrespective of the equipment causing the attrition. Another model proposed by Ghadiri and Zhang[264] models particle damage via a chipping mechanism rather than fracture as in the previous approaches. The chipping results in surface damage that is assumed to be a function of impact velocity and the particle size, hardness, and critical stress intensity. Ghadiri et al.[265,266] also model both the fracture and chipping of particulates. It is found that chipping occurs at low impact velocities while fracture occurs at higher values.

Discrete element methods have also been used to model the dynamics of granular material and/or grinding media in comminution devices. Several studies have focused only on such dynamics and have not considered breakage of the particulate material.[267–270] Other work has incorporated a fragmentation or chipping model discussed above into a DEM simulation of particulate motion in a comminution device. These simulations have modeled breakage of nonporous agglomerates in various devices including a shear cell,[271] a semiautogenous (SAG) mill,[272] and a Hicom mill.[273] Similar work has incorporated Ghadiri's models for particle breakage and chipping in studies of shear deformation[274] and jet milling.[275]

Compression

Various aspects relating to tablet compression have been thoroughly studied using DEM techniques. The process of die filling[140,152,166,276–278] is one aspect that has been studied in both the pharmaceutical and powder metallurgy industries. These studies typically describe the fill rate and particle flow field into a die and make comparisons with experimental results. Other results show the effects of powder characteristics such as friction,[140,152,278] particle-to-die size ratio,[152] effect of shoe speed,[140] and the effect of air pressure.[140,166] The compression of materials within a die has been studied[139,279–285] while others have investigated compression in a periodic system to eliminate die wall effects.[286–288] Rearrangement of particles during the compaction process has also been shown to be important.[75,283,289,290] In much of the compression work, the finite element method (FEM) has been coupled with DEM models so that systems with large particle deformations and large relative densities can be modeled.[139,280,281,283,285,291] This approach permits the modeling of materials with a wide variety of mechanical properties, such as the hardness and ductility, as shown in Figure 12. However, this method is more computationally intensive as individual particles must be meshed and analyzed via FEM.

A few other aspects related to compression have also been approached with DEM modeling. Couroyer et al.[292] used a previously mentioned particle fracture model[265] to examine crushing during compression for various material properties. Martin[293] investigated the springback during the unloading process. Springback was shown to be affected by the material properties, compaction history, and the die wall. In addition to elasticity, the decohesion of particles previously in contact was also shown to be an important factor during unloading. Sweeney and Martin[294] used DEM to determine the microstructure of a high-density

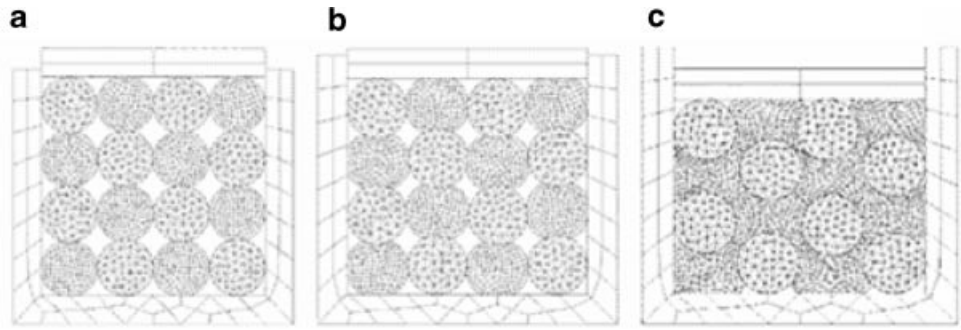

Figure 12. Modeling compression of a mixture of hard and soft ductile materials using a coupled DEM-FEM model. This figure is reprinted from Ransing et al.[285] with permission from The Royal Society.

compact. From this microstructure, they calculated a pore size distribution for varying relative densities that was in good agreement with experimental measurements. Hassanpour and Ghadiri[295] examined the Heckel analysis used for powder compression and determined that it may not be valid for all conditions. Rather, results show it is valid only in a limited range of Young's moduli and yield stresses.

Film Coating

There has been relatively little work published on film coating studies using DEM. Certainly, the results from much of the work with rotating drums discussed in the "Blending" Section can be directly related to the mixing in pan coaters. However, the work by Yamane et al.[296] was one of the first studies to specifically study tablet motion in a pan coater. Inter-tablet uniformity was assessed via the standard deviation of the time each tablet was on the surface as a function of pan loading, particle size, and rotational speed. While the model assumed spherical particles, the results were in qualitative agreement with experimental results. Later DEM work[109] modeled the flow of spheres glued together into two-sphere clusters and performed a detailed comparison with experimental data from a system of mustard seeds obtained with MRI. The particle velocities compared well with those measured experimentally, but only after the coefficient of friction and particle shape (elongation) were adjusted. Further, the model predicted a slightly flatter free surface than was observed experimentally. A similar study by Pandey et al.[176] reported the effect of pan loading and speed on the particle velocities and the dynamic angle of repose. There was good agreement of the particle velocity distributions in the spray zone, and the angles of repose also showed good agreement despite difficulties in measurement of due to the nonlinear surface of the cascading layer.

Additional work related to film coating has looked at different geometries and the assumption of spherical tablets. Nakamura et al.[297] used a coupled DEM-CFD model to assess the inter-tablet coating uniformity in a rotating fluidized bed (RFB) as shown in Figure 13. The RFB coating results were compared with numerical results from a conventional fluidized bed. The RFB was shown to produce significantly less variability in applied coating. Other work has focused on incorporating round convex tablet shapes into DEM models of pan coating equipment.[116]

A different approach has applied the Monte Carlo method to study film coating. Nakamura et al.[14] analyzed the coating uniformity in a tumbling fluidized bed as a function of process conditions using Monte Carlo techniques. Similar work explored the coating uniformity in a Wurster fluidized bed coater.[15] This work showed that an upward cylindrical spray shape better matched experimental results than a solid conical spray shape. It also showed that coating uniformity improved with larger gas velocity and gap height.

CONCLUSIONS

The discrete element method has been used to gain a better understanding of many important processes applicable to the pharmaceutical industry. Several aspects of key operations such as transport, blending, granulation, milling, compression, and film coating have been studied. Work has ranged from fundamental studies in simple geometries that attempt to gain insight into the underlying physics to studies of large process equipment that attempt to elucidate the effects of particle properties and operational parameters on the process.

Historically, DEM models have been limited to a modest number of spherical particles with no interstitial fluid effects. Recent DEM studies, however, are increasingly incorporating nonspherical particles, complex system geometries, noncontact cohesive forces, or interstitial fluid effects via a coupled model with CFD. Additionally, system sizes continue to increase into the hundreds of thousands of particles. Despite the increasing focus on these advanced systems, the effects of nonspherical particles, cohesion, and interstitial air effects are still not well understood. These effects are particularly important for typical pharmaceutical materials, and further study is warranted.

The future of DEM modeling looks very promising. This technique can be used to glean a wide variety of information from many diverse and complex systems comprised of particulate matter as highlighted above. The foremost limitation however, is the vast computational power inherently required which, in turn, limits the number of particles that can be modeled. With the ever increasing power and speed of computers

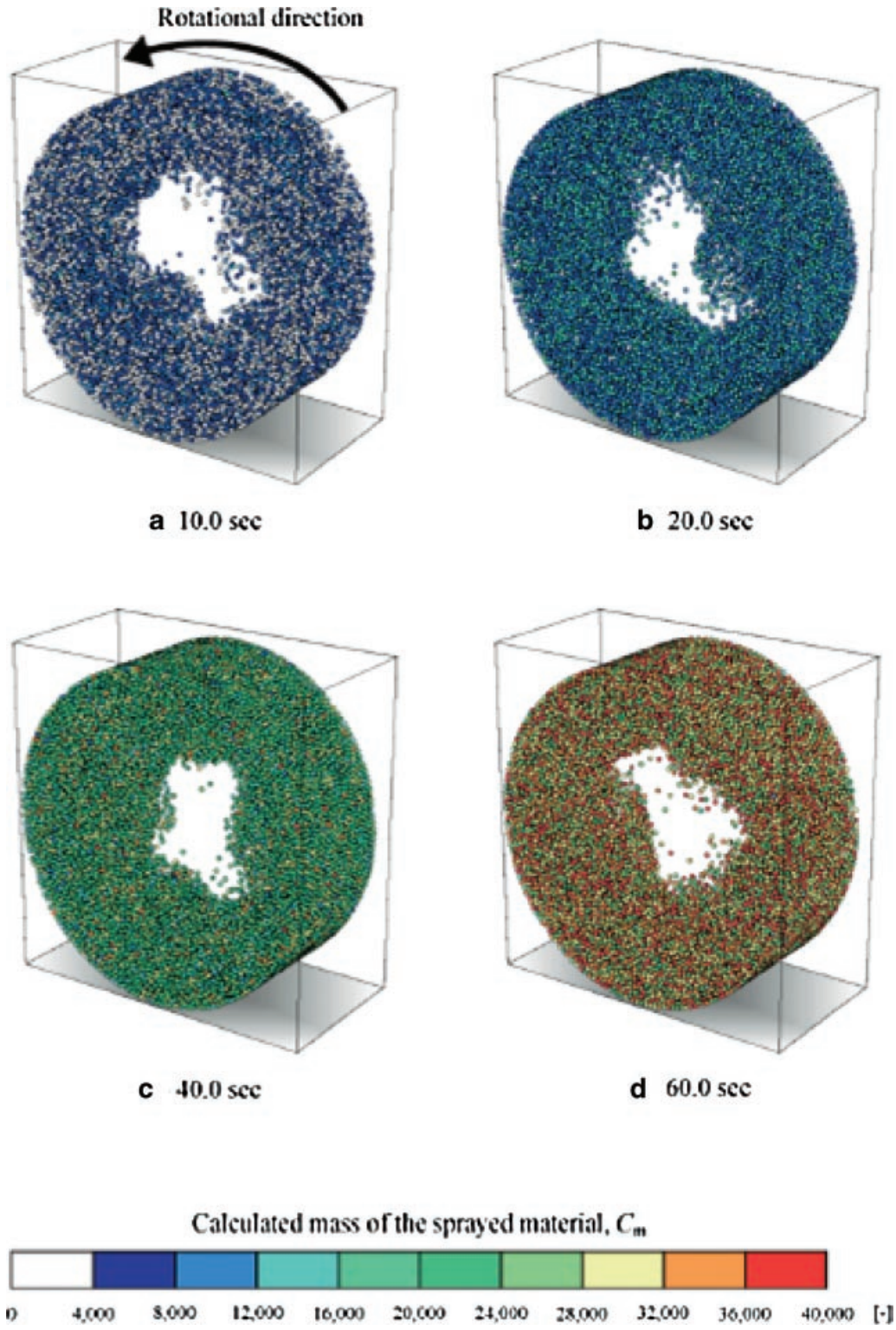

Figure 13. Visualization of the coating mass at four different times in a DEM model of a fluidized bed coater. This figure is reprinted from Nakamura et al.[297] with permission from the Pharmaceutical Society of Japan.

 DOI 10.1002/jps

however, this limitation will become less restrictive. Other concerns, including those that center on the typical assumptions of spherical particles and noncohesive interactions, are the focus of many recent and ongoing studies aimed at developing and refining models that are both accurate and computationally efficient. Incorporation of the results from these efforts will greatly expand the scope of systems that can be quantitatively modeled using DEM, thereby increasing its utility as a predictive design tool.

ACKNOWLEDGMENTS

The authors wish to acknowledge various Pfizer colleagues for their helpful comments and suggestions which have been a great aid during the preparation of this report. Valuable discussions were held with C. Bentham, D. Kremer, M. Mullarney, V. Swaminathan, and N. Turnbull.

REFERENCES

1. Kremer DM, Hancock BC. 2006. Process simulation in the pharmaceutical industry: A review of some basic physical models. J Pharm Sci 95:517–529.
2. Wassgren C, Curtis JS. 2006. The application of computational modeling to pharmaceutical materials science. MRS Bull 31:900–904.
3. Herrmann HJ, Luding S. 1998. Modeling granular media on the computer. Continuum Mech Therm 10:189–231.
4. Zhu HP, Zhou ZY, Yang RY, Yu AB. 2007. Discrete particle simulation of particulate systems: Theoretical developments. Chem Eng Sci 62:3378–3396.
5. Kozicki J, Tejchman J. 2005. Application of a cellular automaton to simulations of granular flows in silos. Granul Matter 7:45–54.
6. LaMarche K, Conway S, Glasser B, Shinbrot T. 2007. Cellular automata model of gravity-driven granular flows. Granul Matter 9:219–229.
7. Yanagita T. 1999. Three-dimensional cellular automaton model of segregation of granular materials in a rotating cylinder. Phys Rev Lett 82:3488.
8. Fitt AD, Wilmott P. 1992. Cellular-automaton model for segregation of a two-species granular flow. Phys Rev A 45:2383–2388.
9. Jullien R, Meakin P, Pavlovitch A. 1992. Three-dimensional model for particle-size segregation by shaking. Phys Rev Lett 69:640.
10. Baxter GW, Behringer RP. 1990. Cellular automata models of granular flow. Phys Rev A 42: 1017–1020.
11. Rosato A, Prinz F, Standburg KJ, Swendsen R. 1986. Monte Carlo simulation of particulate matter segregation. Powder Technol 49:59–69.
12. Rosato AD, Lan Y, Wang DT. 1991. Vibratory particle size sorting in multi-component systems. Powder Technol 66:149–160.
13. Abreu CRA, Tavares FW, Castier M. 2003. Influence of particle shape on the packing and on the segregation of spherocylinders via Monte Carlo simulations. Powder Technol 134:167–180.
14. Nakamura H, Abe E, Yamada N. 1998. Coating mass distributions of seed particles in a tumbling fluidized bed coater. Part II.A. Monte Carlo simulation of particle coating. Powder Technol 99:140–146.
15. KuShaari K, Pandey P, Song Y, Turton R. 2006. Monte Carlo simulations to determine coating uniformity in a Wurster fluidized bed coating process. Powder Technol 166:81–90.
16. Campbell CS, Brennen CE. 1985. Computer simulation of granular shear flows. J Fluid Mech 151: 167–188.
17. Campbell CS, Gong A. 1986. The stress tensor in a two-dimensional granular shear flow. J Fluid Mech 164:107–125.
18. Campbell CS. 1989. The stress tensor for simple shear flows of a granular material. J Fluid Mech 203:449–473.
19. Liss ED, Glasser BJ. 2001. The influence of clusters on the stress in a sheared granular material. Powder Technol 116:116–132.
20. Lasinski ME, Curtis JS, Pekny JF. 2004. Effect of system size on particle-phase stress and microstructure formation. Phys Fluids 16:265–273.
21. Hopkins MA, Louge MY. 1991. Inelastic microstructure in rapid granular flows of smooth disks. Phys Fluids A 3:47–57.
22. Cundall P, Strack ODL. 1979. A discrete numerical model for granular assemblies. Géotechnique 29:47–65.
23. Cleary PW, Sawley ML. 2002. DEM modelling of industrial granular flows: 3D case studies and the effect of particle shape on hopper discharge. Appl Math Model 26:89–111.
24. Ketterhagen WR, Curtis JS, Wassgren CR. 2005. Stress results from two-dimensional granular shear flow simulations using various collision models. Phys Rev E 71:1–11.
25. Schäfer J, Dippel S, Wolf DE. 1996. Force schemes in simulations of granular materials. J Phys I France 6:5–20.
26. Luding S. 1998. Collisions and contacts between two particles. In: Herrmann HJ, Hovi J-P, Luding S, editors. Physics of dry granular media. 1st ed.

Dordrecht: Kluwer Academic Publishing. p 285–304.
27. Stevens AB, Hrenya CM. 2005. Comparison of soft-sphere models to measurements of collision properties during normal impacts. Powder Technol 154:99–109.
28. Haff PK, Werner BT. 1986. Computer simulation of the mechanical sorting of grains. Powder Technol 48:239–245.
29. Babić M, Shen HH, Shen HT. 1990. The stress tensor in granular shear flows of uniform, deformable disks at high solids concentrations. J Fluid Mech 219:81–118.
30. Schäfer J, Wolf DE. 1995. Bistability in simulated granular flow along corrugated walls. Phys Rev E 51:6154–6157.
31. Potapov AV, Campbell CS. 1996. Computer simulation of hopper flow. Phys Fluids 8:2884–2894.
32. Campbell CS. 2002. Granular shear flows at the elastic limit. J Fluid Mech 465:261–291.
33. Cleary PW. 2004. Large scale industrial DEM modelling. Eng Comput 21:169–204.
34. Hertz H. 1882. Über die Berührung fester elastischer Körper. J dir reine u angew Math 92:136.
35. Johnson KL. 1985. Contact mechanics. 1st ed. New York: Cambridge University Press.
36. Lee J. 1994. Density waves in the flows of granular media. Phys Rev E 49:281–298.
37. Ristow GH, Herrmann HJ. 1994. Density patterns in two-dimensional hoppers. Phys Rev E 50:R5–R8.
38. Zhang J, Hu Z, Ge W, Zhang Y, Li T, Li J. 2004. Application of the discrete approach to the simulation of size segregation in granular chute flow. Ind Eng Chem Res 43:5521–5528.
39. Taguchi Yh. 1992. Powder turbulence: Direct onset of turbulent flow. J Phys France II 2: 2103–2114.
40. Kuwabara G, Kono K. 1987. Restitution coefficient in a collision between two spheres. Jpn J Appl Phys 26:1230–1233.
41. Brilliantov NV, Spahn F, Hertzsch JM, Pöschel T. 1996. Model for collisions in granular gases. Phys Rev E 53:5382–5392.
42. Walton OR, Braun RL. 1986. Viscosity, granular temperature, and stress calculations for shearing assemblies of inelastic, frictional disks. J Rheol 30:949–980.
43. McCarthy JJ, Ottino JM. 1998. Particle dynamics simulation: A hybrid technique applied to granular mixing. Powder Technol 97:91–99.
44. Joseph GG, Geffroy E, Mena B, Walton OR, Huilgol RR. 2000. Simulation of filling and emptying in a hexagonal-shape solar grain silo. Particul Sci Technol 18:309–327.
45. Moakher M, Shinbrot T, Muzzio FJ. 2000. Experimentally validated computations of flow, mixing and segregation of non-cohesive grains in 3D tumbling blenders. Powder Technol 109: 58–71.
46. Ristow GH, Herrmann HJ. 1995. Forces on the walls and stagnation zones in a hopper filled with granular material. Physica A 213:474–481.
47. Ristow GH. 1997. Outflow rate and wall stress for two-dimensional hoppers. Physica A 235:319–326.
48. Matuttis HG, Luding S, Herrmann HJ. 2000. Discrete element simulations of dense packings and heaps made of spherical and non-spherical particles. Powder Technol 109:278–292.
49. Mindlin RD, Deresiewicz H. 1953. Elastic spheres in contact under varying oblique forces. J Appl Mech—Trans ASME 20:327–344.
50. Vu-Quoc L, Zhang X, Walton OR. 2000. A 3-D discrete-element method for dry granular flows of ellipsoidal particles. Comput Methods Appl Mech Eng 187:483–528.
51. Seville JPK, Willett CD, Knight PC. 2000. Interparticle forces in fluidisation: A review. Powder Technol 113:261–268.
52. Gröger T, Tüzün U, Heyes DM. 2003. Modelling and measuring of cohesion in wet granular materials. Powder Technol 133:203–215.
53. Baxter J, Abou-Chakra H, Tüzün U, Lamptey BM. 2000. A DEM simulation and experimental strategy for solving fine powder flow problems. Trans Inst Chem Eng 78:1019–1025.
54. Mikami T, Kamiya H, Horio M. 1998. Numerical simulation of cohesive powder behavior in a fluidized bed. Chem Eng Sci 53:1927–1940.
55. Nase ST, Vargas WL, Abatan AA, McCarthy JJ. 2001. Discrete characterization tools for cohesive granular material. Powder Technol 116:214–223.
56. Asmar BN, Langston PA, Matchett AJ, Walters JK. 2002. Validation tests on a distinct element model of vibrating cohesive particle systems. Comput Chem Eng 26:785–802.
57. Asmar BN, Langston PA, Matchett AJ, Walters JK. 2003. Energy monitoring in distinct element models of particle systems. Adv Powder Technol 14:43–69.
58. Rhodes MJ, Wang XS, Nguyen M, Stewart P, Liffman K. 2001. Onset of cohesive behaviour in gas fluidized beds: A numerical study using DEM simulation. Chem Eng Sci 56:4433–4438.
59. Pandit JK, Wang XS, Rhodes MJ. 2006. On Geldart Group A behaviour in fluidized beds with and without cohesive interparticle forces: A DEM study. Powder Technol 164:130–138.
60. Pandit JK, Wang XS, Rhodes MJ. 2007. A DEM study of bubble formation in Group B fluidized beds with and without cohesive inter-particle forces. Chem Eng Sci 62:159–166.
61. Weber MW, Hoffman DK, Hrenya CM. 2004. Discrete-particle simulations of cohesive granular flow using a square-well potential. Granul Matter 6:239–254.

62. Alexander AW, Chaudhuri B, Faqih AM, Muzzio FJ, Davies C, Tomassone MS. 2006. Avalanching flow of cohesive powders. Powder Technol 164:13–21.
63. Weber MW, Hrenya CM. 2006. Square-well model for cohesion in fluidized beds. Chem Eng Sci 61: 4511–4527.
64. Matuttis HG, Schinner A. 2001. Particle simulation of cohesive granular materials. Int J Mod Phys C 12:1011–1021.
65. Fisher RA. 1926. On the capillary forces in an ideal soil. J Agric Sci 16:492–505.
66. Lian G, Thornton C, Adams MJ. 1993. A theoretical study of the liquid bridge forces between two rigid spherical bodies. J Colloid Interfacial Sci 161:138–147.
67. Yang RY, Zou RP, Yu AB. 2003. Numerical study of the packing of wet coarse uniform spheres. AIChE J 49:1656–1666.
68. Yang SC, Hsiau SS. 2001. The simulation of powders with liquid bridges in a 2D vibrated bed. Chem Eng Sci 56:6837–6849.
69. McCarthy JJ. 2003. Micro-modeling of cohesive mixing processes. Powder Technol 138:63–67.
70. Muguruma Y, Tanaka T, Tsuji Y. 2000. Numerical simulation of particulate flow with liquid bridge between particles (simulation of centrifugal tumbling blender). Powder Technol 109:49–57.
71. Soulié F, Cherblanc F, El Youssoufi MS, Saix C. 2006. Influence of liquid bridges on the mechanical behaviour of polydisperse granular materials. Int J Numer Anal Methods Geomech 30:213–228.
72. Richefeu V, El Youssoufi MS, Radjai F. 2006. Shear strength properties of wet granular materials. Phys Rev E 73:051304.
73. Jain K, Shi D, McCarthy JJ. 2004. Discrete characterization of cohesion in gas–solid flows. Powder Technol 146:160–167.
74. Anand A, Curtis JS, Wassgren CR, Hancock BC. 2007. AIChE annual meeting, Salt Lake City, UT.
75. Yen KZY, Chaki TK. 1992. A dynamic simulation of particle rearrangement in powder packings with realistic interactions. J Appl Phys 71:3164–3173.
76. Ye M, van der Hoef MA, Kuipers JAM. 2004. A numerical study of fluidization behavior of Geldart. A particles using a discrete particle model. Powder Technol 139:129–139.
77. Tatemoto Y, Mawatari Y, Noda K. 2005. Numerical simulation of cohesive particle motion in vibrated fluidized bed. Chem Eng Sci 60:5010–5021.
78. Moon SJ, Kevrekidis IG, Sundaresan S. 2006. Particle simulation of vibrated gas-fluidized beds of cohesive fine powders. Ind Eng Chem Res 45: 6966–6977.
79. Thornton C, Yin KK. 1991. Impact of elastic spheres with and without adhesion. Powder Technol 65:153–166.
80. Thornton C, Yin KK, Adams MJ. 1996. Numerical simulation of the impact fracture and fragmentation of agglomerates. J Phys D 29:424–435.
81. Derjaguin BV, Landau LD. 1941. Theory of the stability of strongly charged lyophobic sols and the adhesion of strongly charged particles in solutions of electrolytes. Acta Physicochim (USSR) 14:633–662.
82. Verwey EJW, Overbeek JTG. 1948. Theory of the stability of lyophobic colloids. 1st ed. Amsterdam: Elsevier.
83. Johnson KL, Kendall K, Roberts AD. 1971. Surface energy and the contact of elastic solids. Proc R Soc Lond A 324:301–313.
84. Hong C-W. 1997. New concept for simulating particle packing in colloidal forming processes. J Am Ceram Soc 80:2517–2524.
85. Iwai T, Bezold A, Cordelair J, Greil P. 2001. DEM simulation of colloidal suspension under shear flow Ceram Trans. 112:429–434.
86. Cordelair J, Greil P. 2004. Discrete element modeling of solid formation during electrophoretic deposition. J Mater Sci 39:1017–1021.
87. Gallas JAC, Sokolowski S. 1993. Grain non-sphericity effects on the angle of repose of granular material. Int J Mod Phys B 7:2037–2046.
88. Pöschel T, Buchholtz V. 1993. Static friction phenomena in granular materials: Coulomb law versus particle geometry. Phys Rev Lett 71:3963.
89. Rothenburg L, Bathurst RJ. 1992. Micromechanical features of granular materials with planar elliptical particles. Géotechnique 42:79–7995.
90. Ting JM, Meachum L, Rowell JD. 1995. Effect of particle shape on the strength and deformation mechanisms of ellipse-shaped granular assemblages. Eng Comput 12:99–108.
91. Oda M, Konishi J, Nemat-Nasser S. 1983. Experimental micromechanical evaluation of the strength of granular materials: Effects of particle rolling. In: Jenkins JT, Satake M, editors. Mechanics of granular materials: New models and constitutive relations Amsterdam: Elsevier. p 21–30.
92. Lin X, Ng TT. 1995. Contact detection algorithms for three-dimensional ellipsoids in discrete element modelling. Int J Numer Anal Methods Geomech 19:653–659.
93. Mair K, Frye KM, Marone C. 2002. Influence of grain characteristics on the friction of granular shear zones. J Geophys Res 107:2219.
94. Ting JM, Corkum BT. 1989. Discrete numerical model for soil mechanics. J Geotech Eng 115:379–3398.
95. Morgan JK. 2004. Particle dynamics simulations of rate- and state-dependent frictional sliding of

granular fault gouge. Pure Appl Geophys 161: 1877–1891.
96. Ng TT, Dorby R. 1992. A non-linear numerical model for soil mechanics. Int J Numer Anal Methods Geomech 16:247–263.
97. Ng TT, Dorby R. 1994. Numerical simulations of monotonic and cyclic loading of granular soil. J Geotech Eng 120:388–403.
98. Suiker ASJ, Fleck NA. 2004. Frictional collapse of granular assemblies. J Appl Mech 71:350–358.
99. Iwashita K, Oda M. 1998. Rolling resistance at contacts in simulation of shear band development by DEM. J Eng Mech 124:285–292.
100. Zhou YC, Wright BD, Yang RY, Xu BH, Yu AB. 1999. Rolling friction in the dynamic simulation of sandpile formation. Physica A 269:536–553.
101. Ketterhagen WR, Curtis JS, Wassgren CR, Hancock BC. 2008. Modeling granular segregation in flow from quasi-three-dimensional, wedge-shaped hoppers. Powder Technol 179:126–143.
102. Džiugys A, Peters B. 2001. An approach to simulate the motion of spherical and non-spherical fuel particles in combustion chambers. Granul Matter 3:231–265.
103. Hogue C. 1998. Shape representation and contact detection for discrete element simulations of arbitrary geometries. Eng Comput 15:374–390.
104. Thomas PA, Bray JD. 1999. Capturing non-spherical shape of granular media with disk clusters. J Geotech Geoenviron Eng 125:169–178.
105. Jensen RP, Edil TB, Bosscher PJ, Plesha ME, Khala NB. 2001. Effect of particle shape on interface behavior of DEM-simulated granular materials. Int J Geomech 1:1–19.
106. Allen MP, Imbierski AA. 1987. A molecular dynamics study of the hard dumb-bell system. Mol Phys 60:453–473.
107. Evans KE, Ferrar MD. 1989. The packing of thick fibres. J Phys D 22:354–360.
108. Walton OR, Braun RL, 1993. Joint DOE/NSF workshop on flow of particulates, fluids Ithaca, NY, p 131–148.
109. Yamane K, Nakagawa M, Altobelli SA, Tanaka T, Tsuji Y. 1998. Steady particulate flows in a horizontal rotating cylinder. Phys Fluids 10:1419–1427.
110. Favier JF, Abbaspour-Fard MH, Kremmer M, Raji AO. 1999. Shape representation of axisymmetrical, non-spherical particles in discrete element simulation using multi-element model particles. Eng Comput 16:467–480.
111. Favier JF, Abbaspour-Fard MH, Kremmer M. 2001. Modeling non-spherical particles using multisphere discrete elements. J Eng Mech 127: 971–977.
112. Abou-Chakra H, Baxter J, Tüzün U. 2004. Three-dimensional particle shape descriptors for computer simulation of non-spherical particulate assemblies. Adv Powder Technol 15:63–77.
113. Calantoni J, Todd Holland K, Drake TG. 2004. Modelling sheet-flow sediment transport in wave-bottom boundary layers using discrete-element modelling. Phil Trans R Soc A 362:1987–2001.
114. Buchholtz V, Pöschel T, Tillemans H-J. 1995. Simulation of rotating drum experiments using non-circular particles. Physica A 216:199–212.
115. Tillemans H-J, Herrmann HJ. 1995. Simulating deformations of granular solids under shear. Physica A 217:261–288.
116. Song Y, Turton R, Kayihan F. 2006. Contact detection algorithms for DEM simulations of tablet-shaped particles. Powder Technol 161:32–40.
117. Serra J. 1986. Introduction to mathematical morphology. Comput Vis Graph Image Process 35: 283–305.
118. Rebertus DW, Sando KM. 1977. Molecular dynamics simulation of a fluid of hard spherocylinders. J Chem Phys 67:2585–2590.
119. Munjiza A, Latham JP, John NWM. 2003. 3D dynamics of discrete element systems comprising irregular discrete elements—Integration solution for finite rotations in3D. Int J Numer Methods Eng 56:35–55.
120. Williams SR, Philipse AP. 2003. Random packing of spheres and spherocylinders simulated by mechanical contraction. Phys Rev E 67:051301–051309.
121. Hopkins MA. 2004. Discrete element modeling with dilated particles. Eng Comput 21:422–430.
122. Langston PA, Al-Awamleh MA, Fraige FY, Asmar BN. 2004. Distinct element modelling of non-spherical frictionless particle flow. Chem Eng Sci 59: 425–435.
123. Li J, Langston PA, Webb C, Dyakowski T. 2004. Flow of sphero-disc particles in rectangular hoppers—A DEM and experimental comparison in3D. Chem Eng Sci 59:5917–5929.
124. Rothenburg L, Bathurst RJ. 1991. Numerical simulation of idealized granular assemblies with plane elliptical particles. Comput Geotech 11:315–329.
125. Ting JM. 1992. A robust algorithm for ellipse-based discrete element modelling of granular materials. Comput Geotech 13:175–186.
126. Ting JM, Khwaja M, Meachum L, Rowell JD. 1993. An ellipse-based discrete element model for granular materials. Int J Numer Anal Methods Geomech 17:603–623.
127. Džiugys A, Peters B. 2001. A new approach to detect the contact of two-dimensional elliptical particles. Int J Numer Anal Methods 25:1487–1500.

128. Lin X, Ng TT. 1997. A three-dimensional discrete element model using arrays of ellipsoids. Géotechnique 47:319–329.
129. Ouadfel H, Rothenburg L. 1999. An algorithm for detecting inter-ellipsoid contacts. Comput Geotech 24:245–263.
130. Mustoe GGW, Miyata M. 2001. Material flow analysis of noncircular-shaped granular media using discrete element methods. J Eng Mech 127:1017–1026.
131. Pentland AP, Williams J. 1989. Good vibrations: Modal dynamics for graphics and animation. Comput Graphics 23:215–222.
132. Williams JR, Pentland AP. 1992. Superquadrics and modal dynamics for discrete elements in interactive design. Eng Comput 9:115–127.
133. Cleary PW. 2000. DEM simulation of industrial particle flows: Case studies of dragline excavators, mixing in tumblers and centrifugal mills. Powder Technol 109:83–104.
134. Han K, Feng YT, Owen DRJ. 2006. Polygon-based contact resolution for superquadrics. Int J Numer Methods Eng 66:485–501.
135. Cleary PW. 2007. DEM modelling of particulate flow in a screw feeder. Progr Comput Fluid Dynam 7:128–138.
136. Kohring GA, Melin S, Puhl H, Tillemans HJ, Vermöhlin W. 1995. Computer simulations of critical, non-stationary granular flow through a hopper. Comput Methods Appl Mech Eng 124:273–281.
137. Williams JR, O'Connor R. 1995. A linear complexity intersection algorithm for discrete element simulation of arbitrary geometries. Eng Comput 12:185–201.
138. Nouguier-Lehon C, Cambou B, Vincens E. 2003. Influence of particle shape and angularity on the behavior of granular materials: A numerical analysis. Int J Numer Anal Methods Geomech 27: 1207–1226.
139. Lewis RW, Gethin DT, Yang XS, Rowe RC. 2005. A combined finite-discrete element method for simulating pharmaceutical powder tableting. Int J Numer Methods Eng 62:853–869.
140. Wu C-Y, Cocks ACF. 2006. Numerical and experimental investigations of the flow of powder into a confined space. Mech Mater 38:304–324.
141. Cundall PA. 1988. Formulation of a three-dimensional distinct element model. Part I.A. Scheme to detect and represent contacts in a system composed of many polyhedral blocks. Int J Rock Mech Miner 25:107–116.
142. Hart R, Cundall PA, Lemos J. 1988. Formulation of a three-dimensional distinct element model. Part II. Mechanical calculations for motion and interaction of a system composed of many polyhedral blocks. Int J Rock Mech Miner Sci Geomech Abstr 25:117–125.
143. Ghaboussi J, Barbosa R. 1990. Three-dimensional discrete element method for granular materials. Int J Numer Anal Methods Geomech 14:451–472.
144. Latham JP, Munjiza A. 2004. The modelling of particle systems with real shapes. Phil Trans R Soc Lond A 362:1953–1972.
145. Zhao D, Nezami EG, Hashash YMA, Ghaboussi J. 2006. Three-dimensional discrete element simulation for granular materials. Eng Comput 23:749–770.
146. Pöschel T, Buchholtz V. 1995. Molecular dynamics of arbitrarily shaped granular particles. J Phys I France 5:1431–1455.
147. Potapov AV, Campbell CS. 1998. A fast model for the simulation of non-round particles. Granul Matter 1:9–14.
148. Wang C-Y, Wang C-F, Sheng J. 1999. A packing generation scheme for the granular assemblies with 3D ellipsoidal particles. Int J Numer Anal Methods Geomech 23:815–828.
149. Kuhn MR. 2003. Smooth convex three-dimensional particle for the discrete element method. J Eng Mech 129:539–547.
150. Antony SJ, Kuhn MR. 2004. Influence of particle shape on granular contact signatures and shear strength: New insights from simulations. Int J Solids Struct 41:5863–5870.
151. Hogue C, Newland D. 1994. Efficient computer simulation of moving granular particles. Powder Technol 78:51–66.
152. Wu C-Y, Cocks ACF, Gillia OT, Thompson DA. 2003. Experimental and numerical investigations of powder transfer. Powder Technol 138:216–228.
153. Song Y. 2006. Study of the dynamic behavior of tablet movement in a rotating drum using discrete element modeling (DEM) method. PhD Dissertation. Morgantown, West Virginia: West Virginia University.
154. Langston PA, Tüzün U, Heyes DM. 1996. Distinct element simulation of interstitial air effects in axially symmetric granular flows in hoppers. Chem Eng Sci 51:873–891.
155. Hoomans BPB, Kuipers JAM, Briels WJ, van Swaaij WPM. 1996. Discrete particle simulation of bubble and slug formation in a two-dimensional gas-fluidised bed: A hard-sphere approach. Chem Eng Sci 51:99–118.
156. Tsuji Y, Kawaguchi T, Tanaka T. 1993. Discrete particle simulation of two-dimensional fluidized bed. Powder Technol 77:79–87.
157. Deen NG, Van Sint Annaland M, Van der Hoef MA, Kuipers JAM. 2007. Review of discrete particle modeling of fluidized beds. Chem Eng Sci 62:28–44.
158. Xu BH, Yu AB. 1997. Numerical simulation of the gas–solid flow in a fluidized bed by combining

discrete particle method with computational fluid dynamics. Chem Eng Sci 52:2785–2809.
159. Kawaguchi T, Tanaka T, Tsuji Y. 1998. Numerical simulation of two-dimensional fluidized beds using the discrete element method (comparison between the two- and three-dimensional models). Powder Technol 96:129–138.
160. Li Y, Zhang J, Fan L-S. 1999. Numerical simulation of gas–liquid–solid fluidization systems using a combined CFD–VOF–DPM method: Bubble wake behavior. Chem Eng Sci 54:5101–5107.
161. Rhodes MJ, Wang XS, Nguyen M, Stewart P, Liffman K. 2001. Study of mixing in gas-fluidized beds using a DEM model. Chem Eng Sci 56:2859–2866.
162. van Wachem BGM, van der Schaaf J, Schouten JC, Krishna R, van den Bleek CM. 2001. Experimental validation of Lagrangian–Eulerian simulations of fluidized beds. Powder Technol 116: 155–165.
163. Takeuchi S, Wang S, Rhodes MJ. 2004. Discrete element simulation of a flat-bottomed spouted bed in the 3-D cylindrical coordinate system. Chem Eng Sci 59:3495–3504.
164. Takeuchi S, Shan Wang X, Rhodes MJ. 2005. Discrete element study of particle circulation in a 3-D spouted bed. Chem Eng Sci 60:1267–1276.
165. Rhodes MJ, Wang XS, Nguyen M, Stewart P, Liffman K. 2001. Use of discrete element method simulation in studying fluidization characteristics: Influence of interparticle force. Chem Eng Sci 56:69–76.
166. Wu C-Y, Cocks ACF, Gillia OT. 2003. Die filling and powder transfer. Int J Powder Metall 39:51–64.
167. Tsuji Y, Tanaka T, Ishida T. 1992. Lagrangian numerical simulation of plug flow of cohesionless particles in a horizontal pipe. Powder Technol 71:239–250.
168. Lim EWC, Wang C-H, Yu A-B. 2006. Discrete element simulation for pneumatic conveying of granular material. AIChE J 52:496–509.
169. Zhang Y, Lim EWC, Wang CH. 2007. Pneumatic transport of granular materials in an inclined conveying pipe: Comparison of computational fluid dynamics–discrete element method (CFD–DEM), electrical capacitance tomography (ECT), and particle image velocimetry (PIV) results. Ind Eng Chem Res.
170. Roache PJ. 1998. Verification and validation in computer science and engineering. 1st ed. Albuquerque: Hermosa.
171. Roache PJ, Ghia KN, White FM. 1986. Editorial policy statement on the control of numerical accuracy. J Fluids Eng—Trans ASME 108:2.
172. Freitas CJ. 1993. Editorial policy statement in the control of numerical accuracy. J Fluids Eng—Trans ASME 115:339–340.
173. Grace JR, Taghipour F. 2004. Verification and validation of CFD models and dynamic similarity for fluidized beds. Powder Technol 139:99–110.
174. McCarthy JJ, Shinbrot T, Metcalfe G, Wolf JE, Ottino JM. 1996. Mixing of granular materials in slowly rotated containers. AIChE J 42:3351–3363.
175. Wightman C, Moakher M, Muzzio FJ, Walton O. 1998. Simulation of flow and mixing of particles in a rotating and rocking cylinder. AIChE J 44:1266–1276.
176. Pandey P, Song Y, Kayihan F, Turton R. 2006. Simulation of particle movement in a pan coating device using discrete element modeling and its comparison with video-imaging experiments. Powder Technol 161:79–88.
177. Venugopal R, Rajamani RK. 2001. 3D simulation of charge motion in tumbling mills by the discrete element method. Powder Technol 115:157–166.
178. Medved M, Dawson D, Jaeger HM, Nagel SR. 1999. Convection in horizontally vibrated granular material. Chaos 9:691–696.
179. Li Y, Xu Y, Thornton C. 2005. A comparison of discrete element simulations and experiments for 'sandpiles' composed of spherical particles. Powder Technol 160:219–228.
180. Bertrand F, Leclaire LA, Levecque G. 2005. DEM-based models for the mixing of granular materials. Chem Eng Sci 60:2517–2531.
181. Ketterhagen WR. 2006. Modeling granular segregation during hopper discharge. PhD Dissertation. West Lafayette, IN: Purdue University.
182. Beverloo WA, Leniger HA, Van de velde J. 1961. The flow of granular solids through orifices. Chem Eng Sci 15:260–269.
183. Ketterhagen WR, Curtis JS, Wassgren CR, Kong A, Narayan PJ, Hancock BC. 2007. Granular segregation in discharging cylindrical hoppers: A discrete element and experimental study. Chem Eng Sci 62:6423–6439.
184. Fukushima E. 1999. Nuclear magnetic resonance as a tool to study flow. Annu Rev Fluid Mech 31: 95–123.
185. Nakagawa M, Altobelli SA, Caprihan A, Fukushima E, Jeong E-K. 1993. Non-invasive measurements of granular flows by magnetic resonance imaging. Exp Fluids 16:54–60.
186. Langston PA, Nikitidis MS, Tüzün U, Heyes DM, Spyrou NM. 1997. Microstructural simulation and imaging of granular flows in two- and three-dimensional hoppers. Powder Technol 94:59–72.
187. Lin CL, Miller JD. 2002. Cone beam X-ray microtomography—A new facility for three-dimensional analysis of multiphase materials. Miner Metall Proc 19:65–71.

188. Fu X, Dutt M, Bentham AC, Hancock BC, Cameron RE, Elliott JA. 2006. Investigation of particle packing in model pharmaceutical powders using X-ray microtomography and discrete element method. Powder Technol 167:134–140.
189. Stein M, Martin TW, Seville JPK, McNeil PA, Parker DJ. 1997. Positron emission particle tracking: Particle velocities in gas-fluidized beds, mixers and other applications. In: Chaouki J, Larachi F, Dududkovic MP, editors. Non-invasive monitoring of multiphase flows. Amsterdam: Elsevier Science.
190. Stewart RL, Bridgwater J, Zhou YC, Yu AB. 2001. Simulated and measured flow of granules in a bladed mixer—a detailed comparison. Chem Eng Sci 56:5457–5471.
191. Kuo HP, Knight PC, Parker DJ, Adams MJ, Seville JPK. 2004. Discrete element simulations of a high-shear mixer. Adv Powder Technol 15: 297–309.
192. Kuo HP, Knight PC, Parker DJ, Tsuji Y, Adams MJ, Seville JPK. 2002. The influence of DEM simulation parameters on the particle behaviour in a V-mixer. Chem Eng Sci 57:3621–3638.
193. Broadbent CJ, Bridgwater J, Parker DJ, Keningley ST, Knight P. 1993. A phenomenological study of a batch mixer using a positron camera. Powder Technol 76:317–329.
194. Hoomans BPB, Kuipers JAM, Mohd Salleh MA, Stein M, Seville JPK. 2001. Experimental validation of granular dynamics simulations of gas-fluidised beds with homogenous in-flow conditions using Positron Emission Particle Tracking. Powder Technol 116:166–177.
195. Wildman RD, Huntley JM, Parker DJ. 2001. Convection in highly fluidized three-dimensional granular beds. Phys Rev Lett 86:3304–3307.
196. Yamane K. 2004. Discrete-element method application to mixing and segregation model in industrial blending system. J Mater Res 19:623–627.
197. Parisi DR, Masson S, Martinez J. 2004. Partitioned distinct element method simulation of granular flow within industrial silos. J Eng Mech 130:771–779.
198. Lu Z, Negi SC, Jofriet JC. 1997. A numerical model for flow of granular materials in silos. Part 1. Model development. J Agric Eng Res 68:223–229.
199. Portillo PM, Muzzio FJ, Ierapetritou MG. 2007. Hybrid DEM-compartment modeling approach for granular mixing. AIChE J 53:119–128.
200. Walton OR. 1993. Numerical simulation of inclined chute flows of monodisperse, inelastic, frictional spheres. Mech Mater 16:239–247.
201. Baxter J, Tüzün U, Burnell J, Heyes DM. 1997. Granular dynamics simulations of two-dimensional heap formation. Phys Rev E 55:3546–3554.
202. Khakhar DV, Orpe AV, Andresén P, Ottino JM. 1999. Surface flow of granular materials: Model and experiments in heap formation. Chaos 9:594–610.
203. Langston PA, Tüzün U, Heyes DM. 1994. Continuous potential discrete particle simulations of stress and velocity fields in hoppers: Transition from fluid to granular flow. Chem Eng Sci 49: 1259–1275.
204. Langston PA, Tüzün U, Heyes DM. 1995. Discrete element simulation of granular flow in 2D and 3D hoppers: Dependence of discharge rate and wall stress on particle interactions. Chem Eng Sci 50: 967–987.
205. Kano J, Saito F, Shimosaka A, Hidaka J. 1998. Simulation of mass flow rate of particles discharged from hopper by particle element method. J Chem Eng Jpn 31:936–940.
206. Zhu HP, Yu AB. 2004. Steady-state granular flow in a three-dimensional cylindrical hopper with flat bottom: Microscopic analysis. J Phys D 37:1497–1508.
207. Langston PA, Tüzün U, Heyes DM. 1995. Discrete element simulation of internal stress and flow fields in funnel flow hoppers. Powder Technol 85:153–169.
208. Masson S, Martinez J. 2000. Effect of particle mechanical properties on silo flow and stresses from distinct element simulations. Powder Technol 109:164–178.
209. Hirshfeld D, Rapaport DC. 2001. Granular flow from a silo: Discrete-particle simulations in three dimensions. Eur Phys J E 4:193–199.
210. Hunt ML, Weathers RC, Lee AT, Brennen CE, Wassgren CR. 1999. Effects of horizontal vibration on hopper flows of granular materials. Phys Fluids 11:68–75.
211. Wassgren CR, Hunt ML, Freese PJ, Palamara J, Brennen CE. 2002. Effects of vertical vibration on hopper flows of granular material. Phys Fluids 14:3439–3448.
212. Li J, Mason DJ. 2000. A computational investigation of transient heat transfer in pneumatic transport of granular particles. Powder Technol 112: 273–282.
213. Han T, Levy A, Kalman H. 2003. DEM simulation for attrition of salt during dilute-phase pneumatic conveying. Powder Technol 129:92–100.
214. Lim EWC, Zhang Y, Wang C-H. 2006. Effects of an electrostatic field in pneumatic conveying of granular materials through inclined and vertical pipes. Chem Eng Sci 61:7889–7908.
215. Watano S. 2006. Mechanism and control of electrification in pneumatic conveying of powders. Chem Eng Sci 61:2271–2278.
216. Li J, Webb C, Pandiella SS, Campbell GM, Dyakowski T, Cowell A, McGlinchey D. 2005. Solids

deposition in low-velocity slug flow pneumatic conveying. Chem Eng Process 44:167–173.
217. Shimizu Y, Cundall PA. 2001. Three-dimensional DEM simulations of bulk handling by screw conveyors. J Eng Mech 127:864–872.
218. Moysey PA, Thompson MR. 2005. Modelling the solids inflow and solids conveying of single-screw extruders using the discrete element method. Powder Technol 153:95–107.
219. Inoue E, Tsuji T, Kajiwara T, Funatsu K, Nakayama Y. 2006. Simulation for mixing process in the solid conveying zone of a twin-screw extruder. Seikei-Kakou 18:826–830.
220. McCarthy JJ, Khakhar DV, Ottino JM. 2000. Computational studies of granular mixing. Powder Technol 109:72–82.
221. Dury CM, Ristow GH. 1997. Radial segregation in a two-dimensional rotating drum. J Phys I France 7:737–745.
222. Cleary PW, Metcalfe G, Liffman K. 1998. How well do discrete element granular flow models capture the essentials of mixing processes? Appl Math Model 22:995–1008.
223. Li H, McCarthy JJ. 2005. Phase diagrams for cohesive particle mixing and segregation. Phys Rev E 71:021305.
224. Kwapinska M, Saage G, Tsotsas E. 2006. Mixing of particles in rotary drums: A comparison of discrete element simulations with experimental results and penetration models for thermal processes. Powder Technol 161:69–78.
225. Yang RY, Zou RP, Yu AB. 2003. Microdynamic analysis of particle flow in a horizontal rotating drum. Powder Technol 130:138–146.
226. Taberlet N, Richard P, Hinch EJ. 2006. S shape of a granular pile in a rotating drum. Phys Rev E 73:050301/050301–050301/050304.
227. Lemieux M, Bertrand F, Chaouki J, Gosselin P. 2007. Comparative study of the mixing of free-flowing particles in a V-blender and a bin-blender. Chem Eng Sci 62:1783–1802.
228. Lemieux M, Leonard G, Doucet J, Leclaire LA, Viens F, Chaouki J, Bertrand F. 2008. Large-scale numerical investigation of solids mixing in a V-blender using the discrete element method. Powder Technol 181:205–216.
229. Sudah OS, Arratia PE, Alexander A, Muzzio FJ. 2005. Simulation and experiments of mixing and segregation in a tote blender. AIChE J 51:836–844.
230. Arratia PE, Duong N-h, Muzzio FJ, Godbole P, Reynolds S. 2006. A study of the mixing and segregation mechanisms in the Bohle Tote blender via DEM simulations. Powder Technol 164:50–57.
231. Muguruma Y, Tanaka T, Kawatake S, Tsuji Y. 1997. Discrete particle simulation of a rotary vessel mixer with baffles. Powder Technol 93:261–266.
232. Zhou YC, Yu AB, Stewart RL, Bridgwater J. 2004. Microdynamic analysis of the particle flow in a cylindrical bladed mixer. Chem Eng Sci 59:1343–1364.
233. Terashita K, Nishimura T, Natsuyama S. 2002. Optimization of operating conditions in a high-shear mixer using DEM model: Determination of optimal fill level. Chem Pharm Bull 50:1550–1557.
234. Terashita K, Nishimura T, Natsuyama S, Munetake S. 2002. DEM simulation of mixing and segregation in high-shear mixer. J Jpn Soc Powder Metall 49:638–645.
235. Zhou YC, Yu AB, Bridgwater J. 2003. Segregation of binary mixture of particles in a bladed mixer. J Chem Technol Biotechnol 78:187–193.
236. Kaneko Y, Shiojima T, Horio M. 2000. Numerical analysis of particle mixing characteristics in a single helical ribbon agitator using DEM simulation. Powder Technol 108:55–64.
237. Gyenis J. 2002. Motionless mixers in bulk solids treatments—A review. Kona 20:9–23.
238. Gyenis J, Levy A. 2005. Special issue on conveying and handling of particulate solids. Chem Eng Process 44:139–140.
239. Cameron IT, Wang FY, Immanuel CD, Stepanek F. 2005. Process systems modelling and applications in granulation: A review. Chem Eng Sci 60: 3723–3750.
240. Gantt JA, Gatzke EP. 2005. High-shear granulation modeling using a discrete element simulation approach. Powder Technol 156:195–212.
241. Verkoeijen D, Pouw GA, Meesters GMH, Scarlett B. 2002. Population balances for particulate processes—a volume approach. Chem Eng Sci 57:2287–2303.
242. Gantt JA, Cameron IT, Litster JD, Gatzke EP. 2006. Determination of coalescence kernels for high-shear granulation using DEM simulations. Powder Technol 170:53–63.
243. Gantt JA, Gatzke EP. 2006. A stochastic technique for multidimensional granulation modeling. AIChE J 52:3067–3077.
244. Tardos GI, Khan MI, Mort PR. 1997. Critical parameters and limiting conditions in binder granulation of fine powders. Powder Technol 94: 245–258.
245. Moreno-Atanasio R, Ghadiri M. 2006. Mechanistic analysis and computer simulation of impact breakage of agglomerates: Effect of surface energy. Chem Eng Sci 61:2476–2481.
246. Lian G, Thornton C, Adams MJ. 1998. Discrete particle simulation of agglomerate impact coalescence. Chem Eng Sci 53:3381–3391.
247. Goldschmidt MJV, Weijers GGC, Boerefijn R, Kuipers JAM. 2003. Discrete element modelling of fluidised bed spray granulation. Powder Technol 138:39–45.

248. Talu I, Tardos GI, Khan MI. 2000. Computer simulation of wet granulation. Powder Technol 110:59–75.
249. Mishra BK, Thornton C, Bhimji D. 2002. A preliminary numerical investigation of agglomeration in a rotary drum. Miner Eng 15:27–33.
250. Link JM, Godlieb W, Deen NG, Kuipers JAM. 2007. Discrete element study of granulation in a spout-fluidized bed. Chem Eng Sci 62:195–207.
251. Odagi K, Tanaka T, Tsuji Y. 2001. Compressive flow properties of powder in roll-type presses—numerical simulation by discrete element method. J Soc Powder Technol Jpn 38:150–159.
252. Dec RT, Zavaliangos A, Cunningham JC. 2003. Comparison of various modeling methods for analysis of powder compaction in roller press. Powder Technol 130:265–271.
253. Horio M. 2003. Binderless granulation—its potential, achievements and future issues. Powder Technol 130:1–7.
254. Potapov AV, Campbell CS. 1994. Computer simulation of impact-induced particle breakage. Powder Technol 81:207–216.
255. Potapov AV, Hopkins MA, Campbell CS. 1995. A two-dimensional dynamic simulation of solid fracture. Part I. Description of the model. Int J Mod Phys C 6:371–398.
256. Potapov AV, Campbell CS, Hopkins MA. 1995. A two-dimensional dynamic simulation of solid fracture. Part II. Examples. Int J Mod Phys C 6:399–425.
257. Kun F, Herrmann HJ. 1996. Fragmentation of colliding discs. Int J Mod Phys C 7:837–855.
258. Ning Z, Boerefijn R, Ghadiri M, Thornton C. 1997. Distinct element simulation of impact breakage of lactose agglomerates. Adv Powder Technol 8:15–37.
259. Thornton C, Ciomocos MT, Adams MJ. 1999. Numerical simulations of agglomerate impact breakage. Powder Technol 105:74–82.
260. Kafui KD, Thornton C. 2000. Numerical simulations of impact breakage of a spherical crystalline agglomerate. Powder Technol 109:113–132.
261. Golchert D, Moreno R, Ghadiri M, Litster J. 2004. Effect of granule morphology on breakage behaviour during compression. Powder Technol 143-144:84–96.
262. Neil AU, Bridgwater J. 1999. Towards a parameter characterising attrition. Powder Technol 106:37–44.
263. Gwyn JE. 1969. On the particle size distribution function and the attrition of cracking catalysts. AIChE J 15:35–39.
264. Ghadiri M, Zhang Z. 2002. Impact attrition of particulate solids. Part 1. A theoretical model of chipping. Chem Eng Sci 57:3659–3669.
265. Ghadiri M, Ning Z. 1997. Effect of shear strain rate on attrition of particulate solids in a shear cell. In: Behringer RP, Jenkins JT, editors. Powder and grains '97. Rotterdam: Balkema. p 127–130.
266. Papadopoulos DG, Teo CS, Ghadiri M, Bell TA. 1998. World congress on particle technology, vol. 3, Brighton, UK.
267. Mishra BK, Rajamani RK. 1990. Study of media mechanics in tumbling mills by discrete element method. Kona 8:92–98.
268. Rajamani RK, Mishra BK, Venogopal R, Datta A. 2000. Discrete element analysis of tumbling mills. Powder Technol 109:105–112.
269. Cleary PW. 2001. Modelling comminution devices using DEM. Int J Numer Anal Methods Geomech 25:83–105.
270. Jayasundara CT, Yang RY, Yu AB. 2006. Discrete particle simulation of particle flow in the IsaMill process. Ind Eng Chem Res 45:6349–6359.
271. Potapov AV, Campbell CS. 1997. Computer simulation of shear-induced particle attrition. Powder Technol 94:109–122.
272. Herbst JA, Potapov AV. 2004. Making a Discrete Grain Breakage model practical for comminution equipment performance simulation. Powder Technol 143–144:144–150.
273. Hoyer DI. 1999. The discrete element method for fine grinding scale-up in Hicom mills. Powder Technol 105:250–256.
274. Ning Z, Ghadiri M. 2006. Distinct element analysis of attrition of granular solids under shear deformation. Chem Eng Sci 61:5991–6001.
275. Han T, Kalman H, Levy A. 2002. DEM simulation of particle comminution in jet milling. Particul Sci Technol 20:325–340.
276. Coube O, Cocks ACF, Wu CY. 2005. Experimental and numerical study of die filling powder transfer and die compaction. Powder Metall 48: 68–76.
277. Ozaki Y, Uenosono S, Tagami N, Kuwagi K, Noda R, Horio M. 2006. Experimental and numerical investigations of the die filling of iron powders. Adv Powder Metall Particul Mater 3:35–46.
278. Siiriä S, Yliruusi J. 2007. Particle packing simulations based on Newtonian mechanics. Powder Technol 174:82–92.
279. Lian J, Shima S. 1994. Powder assembly simulation by particle dynamics method. Int J Numer Methods Eng 37:763–775.
280. Ransing RS, Gethin DT, Khoei AR, Mosbah P, Lewis RW. 2000. Powder compaction modelling via the discrete and finite element method. Mater Design 21:263–269.
281. Gethin DT, Ransing RS, Lewis RW, Dutko M, Crook AJL. 2001. Numerical comparison of a deformable discrete element model and an equivalent continuum analysis for the compaction of ductile porous material. Comput Struct 79:1287–1294.

282. Odagi K, Tanaka T, Yamane K. 2002. Proc World Cong Part Tech 4.
283. Zavaliangos A. 2002. A multiparticle simulation of powder compaction using finite element discretization of individual particles. Mater Res Soc Symp Proc 731:169–175.
284. Hashimoto H, Sun ZM, Park YH, Abe T. 2003. Model simulation of powder compaction by complex mold based on deformation behavior of free particles measured by compression test. Mater Res Soc Symp Proc 759:41–45.
285. Ransing RS, Lewis RW, Gethin DT. 2004. Using a deformable discrete-element technique to model the compaction behaviour of mixed ductile and brittle particulate systems. Phil Trans R Soc Lond A 362:1867–1884.
286. Martin CL, Bouvard D. 2003. Study of the cold compaction of composite powders by the discrete element method. Acta Mater 51:373–386.
287. Skrinjar O, Larsson P-L. 2004. Cold compaction of composite powders with size ratio. Acta Mater 52: 1871–1884.
288. Sheng Y, Lawrence CJ, Briscoe BJ, Thornton C. 2004. Numerical studies of uniaxial powder compaction process by 3D DEM. Eng Comput 21:304–317.
289. Redanz P, Fleck NA. 2001. The compaction of a random distribution of metal cylinders by the discrete element method. Acta Mater 49:4325–4335.
290. Martin CL, Bouvard D, Shima S. 2003. Study of particle rearrangement during powder compaction by the Discrete Element Method. J Mech Phys Solids 51:667–693.
291. Zavaliangos A, Procopio AT. 2005. Understanding strength of powder compacts using a detailed multi-scale simulation. Adv Powder Metall Particul Mater 1:52–61.
292. Couroyer C, Ning Z, Ghadiri M. 2000. Distinct element analysis of bulk crushing: Effect of particle properties and loading rate. Powder Technol 109:241–254.
293. Martin CL. 2003. Unloading of powder compacts and their resulting tensile strength. Acta Mater 51:4589–4602.
294. Sweeney SM, Martin CL. 2003. Pore size distributions calculated from 3-D images of DEM-simulated powder compacts. Acta Mater 51: 3635–3649.
295. Hassanpour A, Ghadiri M. 2004. Distinct element analysis and experimental evaluation of the Heckel analysis of bulk powder compression. Powder Technol 141:251–261.
296. Yamane K, Sato T, Tanaka T, Tsuji Y. 1995. Computer simulation of tablet motion in coating drum. Pharm Res 12:1264–1268.
297. Nakamura H, Iwasaki T, Watano S. 2006. Numerical simulation of film coating process in a novel rotating fluidized bed. Chem Pharm Bull 54:839–846.
298. Fowler RT, Glastonbury JR. 1959. The flow of granular solids through orifices. Chem Eng Sci 10:150–156.